

**CONSTRUCTION OF HIGH QUALITY
PHARMACOPHORE MODEL FOR THE HUMAN
SKIN PIGMENTATION ENZYME TYROSINASE
AND SUBSEQUENT IN-SILICO AND IN-VITRO
SCREENING FOR NEW TYROSINASE
INHIBITORS**

By

Rushdie Abuhamdah

Supervisor

Dr. Mutasem O. Taha

Co-Supervisor

Dr. Saja Hamed

**This Thesis was Submitted in Partial Fulfillment of the Requirements for the
Master's Degree of Pharmaceutical Sciences**

**Faculty of Graduate Studies
The University of Jordan**

April, 2008

This Thesis (Construction of high quality pharmacophore model for the human skin pigmentation enzyme tyrosinase and subsequent *in-silico* and *in-vitro* screening for new tyrosinase inhibitors) was successfully defended and approved on 27/03/2008

Committee Members

Signature

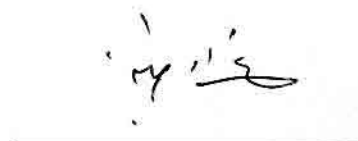
Dr. Mutasem O. Taha, Chairman
Associate Professor of Pharmaceutical Medicinal Chemistry



Dr. Saja Hamed, Co-supervisor,
Assistant Professor of Pharmaceutics and Cosmetic Science



Dr. Ghassan Abu Sheikha, Member
Associate Professor of Pharmaceutical Medicinal Chemistry
(Al-Zaytoonah Private University of Jordan)



Dr. Yasser K. Bustanji, Member
Associate Professor of Biochemistry



Dr. Mohammad K. Laham, Member
Assistant Professor of Medicinal and Biological Chemistry



تعتمد كلية الدراسات العليا
هذه النسخة من الرسالة
التوقيع..... التاريخ: 27/3/08

Dedicated

To

Father, Mother

Brothers and Sisters

Acknowledgements

I would like to express my deep gratitude to Dr. MutasemTaha for his supervision, guidance and encouragement to keep my morale high.

I am indebted to Dr.Saja Hamed for her kind orientation and invaluable remarks and contribution.

I am so much grateful to the members of the Examination Committee for their subtle vision and constructive suggestions.

Last but not least, I would like to extend my hearty greetings to the members of the faculty of Pharmacy at the University of Jordan who gave me support and helpful contribution.

List of Content

Title	Page
Committee decision	ii
Dedication	iii
Acknowledgement	iv
List of content	v
List of tables	vii
List of figures	viii
List of abbreviations	x
Abstract (English)	xi
1. Introduction	1
1.1 The skin	1
1.1.1 Organization and general function	1
1.1.2 Skin melanocytes	2
1.1.3 Melanin	5
1.1.4 Melanin synthetic pathways	6
1.1.5 Microscopic appearance	8
1.1.6 Tyrosinase	9
1.1.6.1 Chemical reaction	9
1.1.6.2 Tyrosinase structure	10
1.1.6.3 Transmembrane protein and sorting	10
1.1.6.4 Active site	10
1.1.7 Skin colour	12

1.1.7.1 Skin depigmenting agents	12
1.8. Drug design and discovery by pharmacophore modeling	17
1.9 Pharmacophore modeling utilizing Catalyst® software package	19
1.9.1 Catalyst® modules	19
1.9.2.1 The generation of multiple conformations	20
1.9.2.2 Pharmacophore hypotheses automated generation	20
1.9.2.3 HypoGen & HipHop	20
1.9.2.4 Three-dimensional database searching	21
1.9.2.5 Database searching using CATALYST/Shape® program	21
1.10 Objectives	22
2. Experimental	23
3. Results and discussion	32
4. Conclusion	44
5. Future work	44
6. References	47
Appendix I	58-59
Abstract (Arabic)	60

List of Tables

Table number	Title	Page
Table 1	The training list used for pharmacophore modeling of tyrosinase inhibitors	40
Table 2	The pharmacophoric features of the 10 hypotheses generated by HipHop Refine automatic run	41
Table 3	Minibiobyte Hits	42
Table 4	Flora Hits	43

List of Figures

Figure number	Title	Page
Figure 1	Schematic drawing of human skin structure	2
Figure 2	Schematic drawing of an epidermal melanin unit showing a melanocyte and the group of keratinocytes with which it maintains functional contacts.	4
Figure 3	Mechanism behind melanosome transfer in melanocytes	4
Figure 4	Metabolic pathway of eumelanin and pheomelanin biosynthesis	7
Figure 5	Fine structure of an epidermal melanocyte after immediate tanning reaction	8
Figure 6	(A) Conversion of tyrosine to melanin(s) (B) Conversion of catechol to benzoquinone	9
Figure 7	Crystal structure of a Streptomyces derived tyrosinase in complex with a so called "caddie protein"	11
Figure 8	The mechanism of skin depigmenting action	14
Figure 9	Chemical structures of hydroquinone , kojic acid, tyrosine and arbutin	15
Figure 10	Chemical structures of the 7 tyrosinase inhibitors applied to HipHopRefine modeling.	36

Figure 11	The pharmacophoric features of (A) Hypo 1 (HBA: hydrogen bond acceptor,) (B) Hypo 1 with added excluded volumes (gray spheres).	37
Figure 12	Mapping the highest ranking pharmacophore model against inhibitor number 5.	38
Figure 13	Mapping the highest ranking pharmacophore model against inhibitor number 4.	39
Figure 14	Percent tyrosinase inhibition by arbutin, 3,4-(methylenedioxy) cinnamic acid and kojic acid	45
Figure 15	Percentage tyrosinase inhibition by <i>A. Cherimola</i>	46

List of Abbreviations

2D	Two-Dimensional
3D	Three-Dimensional
COMFA	Comparative molecular field analysis
IC ₅₀	Inhibitor concentration required for 50% inhibition
HQ	Hydroquinone
MFA	Molecular field analysis
HBA	Hydrogen bond acceptor
HBD	Hydrogen bond doner
CHARMm	Chemistry of harvard molecular mechanics
Arg	Arginine
QSAR	Quantitative structure-activity relationship
Tyr	Tyrosine
NMR	Nuclear magnetic resonance
DHI	5,6-dihydroxyindole
DHICA	5,6-dihydroxyindole-2-carboxylic acid

**CONSTRUCTION OF HIGH QUALITY PHARMACOPHORE
MODEL FOR THE HUMAN SKIN PIGMENTATION ENZYME
TYROSINASE AND SUBSEQUENT IN-SILICO AND IN-VITRO
SCREENING FOR NEW TYROSINASE INHIBITORS**

By

Rushdie Abuhamdah

Supervisor

Dr. Mutasem O. Taha

Co-Supervisor

Dr. Saja Hamad

ABSTRACT

Tyrosinase inhibitors have become increasingly important in medication and in cosmetics to ameliorate skin hyperpigmentation by inhibiting the rate limiting step in melanin synthesis. A number of naturally occurring tyrosinase inhibitors have been described, the majority consisting of a phenol structure or of metal chelating agents. Some of these inhibitors are bound by a number of limitations, such as low activity, high toxicity, and insufficient penetrative ability. For example, arbutin which is a potentially active agent has not yet been demonstrated clinically efficient. Besides, hydroquinone, a widely used skin lightening agent, is cytotoxic to melanocytes and potentially mutagenic.

No previous pharmacophore modeling for tyrosinase enzyme has been found in the literature. The aim of this study is to construct a high quality pharmacophore model for the human skin pigmentation enzyme tyrosinase and subsequent *in-silico* and *in-vitro* screening for the sake of identifying new tyrosinase inhibitors.

The validity of the model was experimentally established by studying mushroom tyrosinase inhibitory activity of 3,4-(Methylenedioxy) cinnamic acid and plant extract of (*Annona cherimola* Mill) selected by the constructed pharmacophore model. 3, 4-(Methylenedioxy) cinnamic acid and plant extract of (*Annona cherimola* Mill) both showed inhibitory activity against mushroom tyrosinase similar to that of arbutin; a well-known tyrosinase inhibitor. These results support the role of *in-silico* model for the identification of new tyrosinase inhibitors.

1. INTRODUCTION

1.1 The skin

1.1.1 Organization and General Function

The skin separates human body from the external environment. It covers the entire surface of the body and is the body's largest organ, accounting for 15 percent of the body weight. In adults, the skin has a surface area of about 1.8 square meters and varies in thickness from 0.5 mm on the eyelids to 5.0 mm or more on the back between the shoulder blades, on the palms of the hands, and on feet soles (Fritsch, 1990).

The skin and skin appendages (hair, nails, and glands) make up the integumentary system. The skin has an outer epidermis and inner dermis. The human epidermis is composed of three cell types: melanocytes, keratinocytes and Langerhans cells (Fritsch, 1990). Melanocytes account for 5% to 10% of the cellular content and are located in the basal layer in the epidermis. The melanocytes produce melanin to protect the skin from UV radiation. After production of melanin in the melanocytes, the melanin is transferred to the keratinocytes, where it becomes visible as a skin colour (Zuidhoff & Rijsbergen, 2001). The dermis is tightly fastened to the epidermis by a basement membrane and to underlying muscles by subcutaneous loose connective tissue (Figure 1).

The skin protects underlying structures against abrasion and dehydration; it also helps in regulating body temperature and maintaining homeostasis through sweating and regulating the amount of blood flow in the dermis. Millions of sensory receptors in the skin receive stimuli from the environment, and the body respond to these stimuli to maintain homeostasis. The skin also plays an important role in immunity and other body defence mechanism (Creager, 1992). In addition, the pigment melanin in the

skin, which is the primary determinant of skin colour, helps in protecting the skin against ultraviolet radiation.

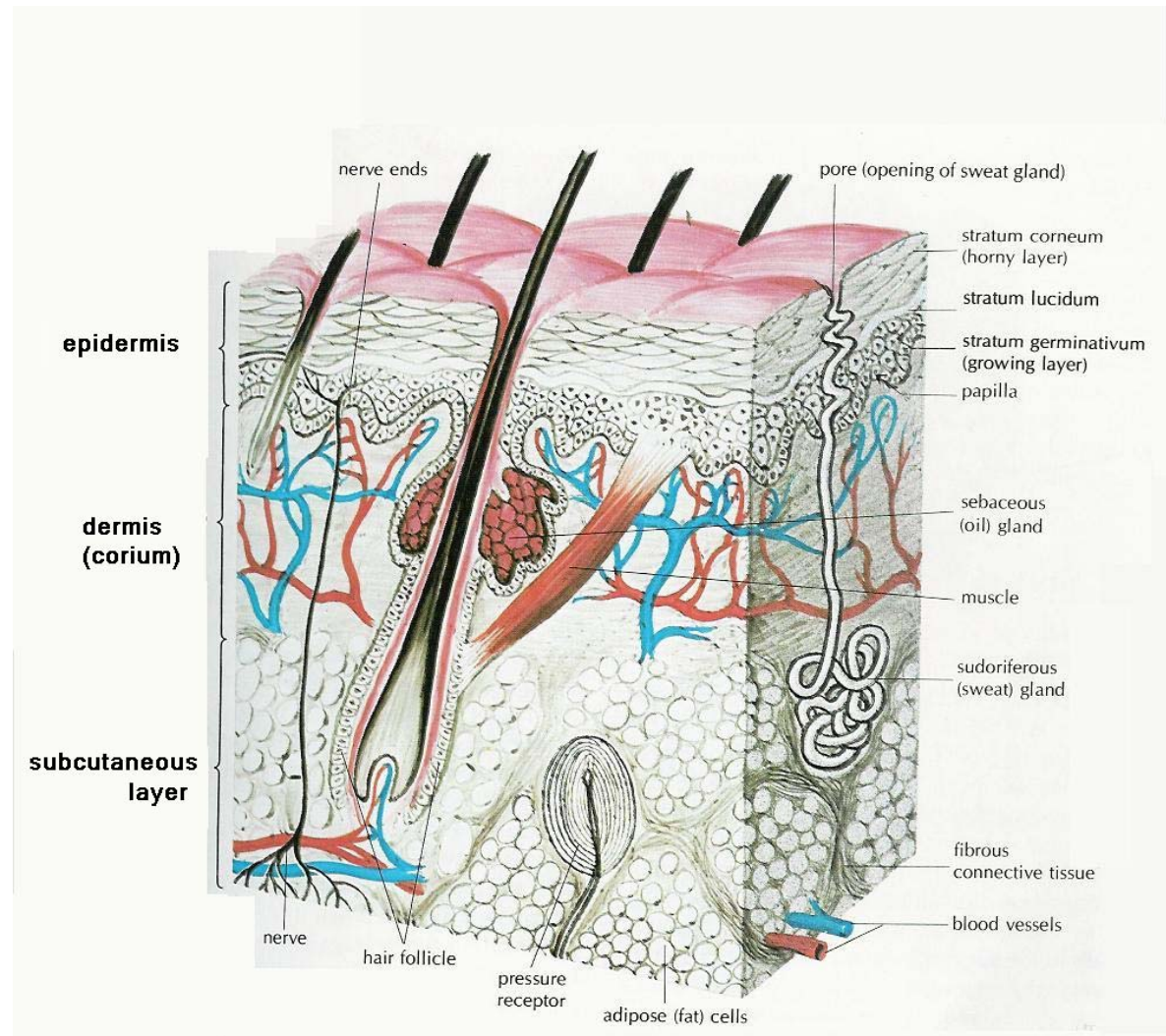


Figure 1: Schematic drawing of human skin structure (Fritsch, 1990).

1.1.2 Skin melanocytes

Skin melanocytes reside at the epidermal/dermal junction, and actively produce and transfer melanin to neighbouring keratinocytes in response to hormonal or external stimuli, notably UV light, which results in skin darkening. Recent studies have shown that melanocytes express numerous cell surface receptors that allow them to interact

with other cells in their microenvironment, including keratinocytes and Langerhans cells (Prota, 1996).

Studies of the mechanism of melanin transfer and distribution suggest that keratinocytes acquire melanin particles by phagocytizing portions of the melanocytes dendrites. It is also possible that keratinocytes play some active role in controlling the rate of melanin synthesis by melanocytes, and that the whole question of pigmentation involves complementary activities by melanocytes and keratinocytes. This has been concisely expressed in the concept of the epidermal melanin unit (Figure 2) proposed by Fitzpatrick & Breathnach (1963) to emphasize the existence of a structural and functional organization of melanocytes and keratinocytes at a biological level higher than of the individual cell (Prota, 1996). Such a view is consistent with a number of observations showing that factors affecting the integrity and proliferation of keratinocytes (such as mechanical injury, heat, UV radiation and inflammation) also have an indirect effect on the morphology and functional state of melanocytes. Indeed, it appears that melanocytes behave as if they know exactly what is going on in the keratinocytes and vice versa and that this knowledge profoundly influences the reciprocal behaviour. The molecular and cellular mechanisms involved in melanosome transfer and the keratinocyte–melanocyte interactions required for this process are not yet completely understood. Suggested mechanisms of melanosome transfer include melanosome release and endocytosis, direct inoculation, keratinocyte–melanocyte membrane fusion, and phagocytosis (Seiberg, 2001).

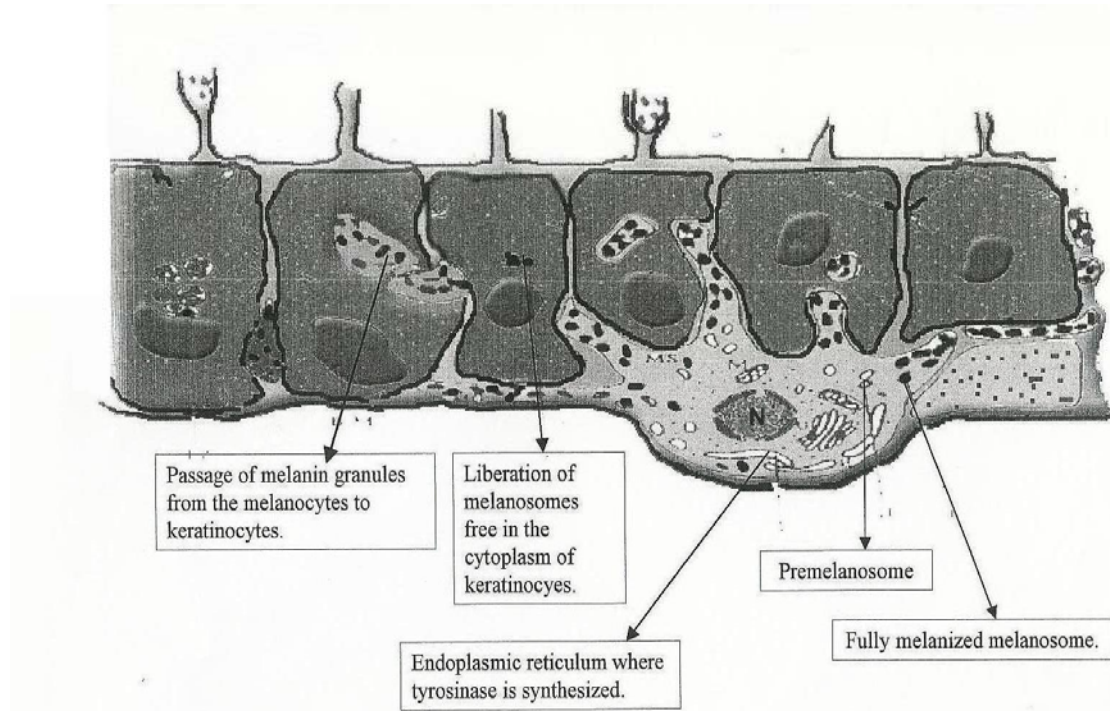
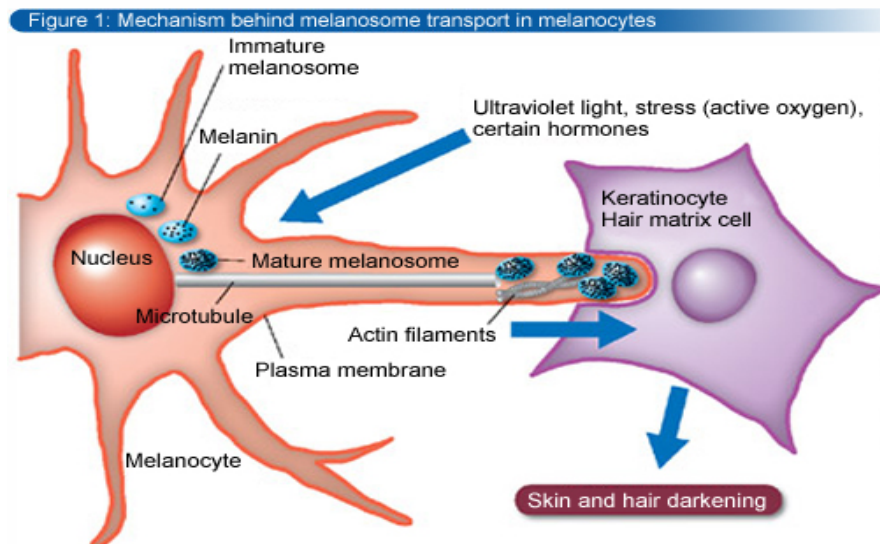


Figure 2: Schematic drawing of an epidermal melanin unit showing a melanocyte and the group of keratinocytes with which it maintains functional contacts.

(Fitzpatrick & Breathnach, 1963)



When melanocytes are activated by ultraviolet light etc., melanin (schematically shown as granules) is formed around the nucleus and stored in small organelles known as melanosomes. Melanosomes are transported along microtubules and actin filaments to the cell periphery. Subsequently, melanosomes bind to the plasma membrane and transfers melanosomes to keratinocytes and hair matrix cells, resulting in skin and hair blackening.

Figure 3: Mechanism behind melanosome transfer in melanocytes

(Quevedo *et al.*, 1987)

Thus, for *in vitro* testing of depigmenting agents uses of bicompartamental coculture system where cell communication between keratinocytes and melanocytes can take place is considered a more reliable experimental design. This experimental situation enables to monitor the effect of biological agents released by both cell types on melanogenesis and the interference of tested compounds with this system.

Melanocytes and keratinocytes co-operate for the transfer and the distribution of melanosomes throughout the epidermis (Figure 3), but it is now well accepted that a number of endogenous agents released from the keratinocytes upon irradiation by UV radiation also modulate the melanogenesis (endothelin-1(ET-1), granulocyte/macrophage colony stimulating factor (GM-CSF), nitric oxide (NO), alpha-melanocytes-stimulating hormone (alpha-MSH), etc.). In fact, the expression of the major enzymes needed for melanin synthesis seems to be regulated by keratinocytes-derived factors (Nicolay & Levrat, 2003).

This understanding of the different communication pathways involved in melanization opens opportunities for new strategies to ameliorate skin pigmentation (e.g. alpha-MSH analogues for skin tanning, NO inhibitor for skin-lightening, etc.).

1.1.3 Melanin

In humans, melanin is found in skin, hair, the pigmented tissue underlying the iris, the medulla and zona reticularis of the adrenal gland, the stria vascularis of the inner ear, and in pigment bearing neurons of certain deep brain nuclei such as the locus ceruleus and the substantia nigra. Dermal melanin is produced by melanocytes, which are found in the stratum basale of the epidermis. Although human beings generally possess a similar concentration of melanocytes in their skin, the melanocytes in some individuals and ethnic groups more frequently or less frequently express the melanin-

producing genes, thereby conferring a greater or lesser concentration of skin melanin. Some individual animals and humans have very little or no melanin in their bodies, a condition known as albinism (Zuidhoff & Rijsbergen, 2001).

Melanin is an aggregate of smaller component molecules that can be categorized into two groups:

Eumelanin: There are two different types of eumelanin, which are distinguished from each other by their pattern of polymer bonds. The two types are black eumelanin and brown eumelanin. (Prota *et al.*, 1998; Zuidhoff & Rijsbergen, 2001).

Pheomelanin imparts a pink to red hue and, thus, is found in particularly large quantities in red hair. Pheomelanin is particularly concentrated in the lips, nipples, glans of the penis, and vagina. Pheomelanin also may become carcinogenic when exposed to the ultraviolet rays of the sun. Chemically, pheomelanin differs from eumelanin in that its oligomer structure incorporates the amino acid L-cysteine, as well as 5,6-dihydroxyindole (DHI) and 5,6-dihydroxyindole-2-carboxylic acid (DHICA) units (Prota *et al.*, 1998).

1. 1.4 Melanin Synthetic Pathways

The first step of the synthetic pathway for both eumelanins and pheomelanins is mediated by tyrosinase (Figure 4):

Tyrosine → DOPA → dopaquinone

Dopaquinone can combine with cysteine by two pathways to benzothiazines and pheomelanins

Dopaquinone + cysteine → 5-S-cysteinyl-dopa → benzothiazine intermediate → pheomelanin

Dopaquinone + cysteine \rightarrow 2-S-cysteinylDOPA \rightarrow benzothiazine intermediate \rightarrow pheomelanin

Alternatively, dopaquinone can be converted to leucodopachrome and follow two more pathways to the eumelanins:

Dopaquinone \rightarrow leucodopachrome \rightarrow dopachrome \rightarrow 5,6-dihydroxyindole-2-carboxylic acid \rightarrow quinone \rightarrow eumelanin

Dopaquinone \rightarrow leucodopachrome \rightarrow dopachrome \rightarrow 5,6-dihydroxyindole \rightarrow quinone \rightarrow eumelanin

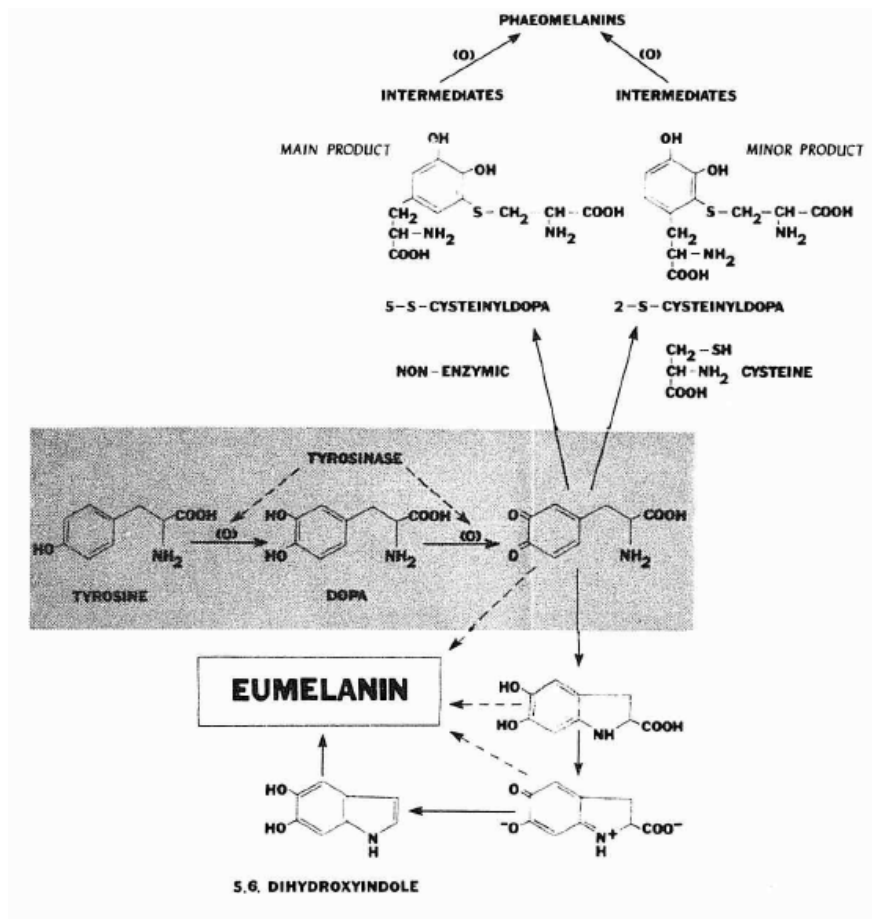


Figure 4: Metabolic pathway of eumelanin and pheomelanin biosynthesis (Prota, 1996)

1.1.5 Microscopic appearance

Under the microscope, melanin is brown, non-refractile and finely granular with individual granules having a diameter of less than 800 nanometers. This differentiates melanin from common blood breakdown pigments which are larger, chunky and refractile and range in color from green to yellow or red-brown. In heavily pigmented lesions, dense aggregates of melanin can obscure histologic detail (Jimbow *et al.*, 1976).

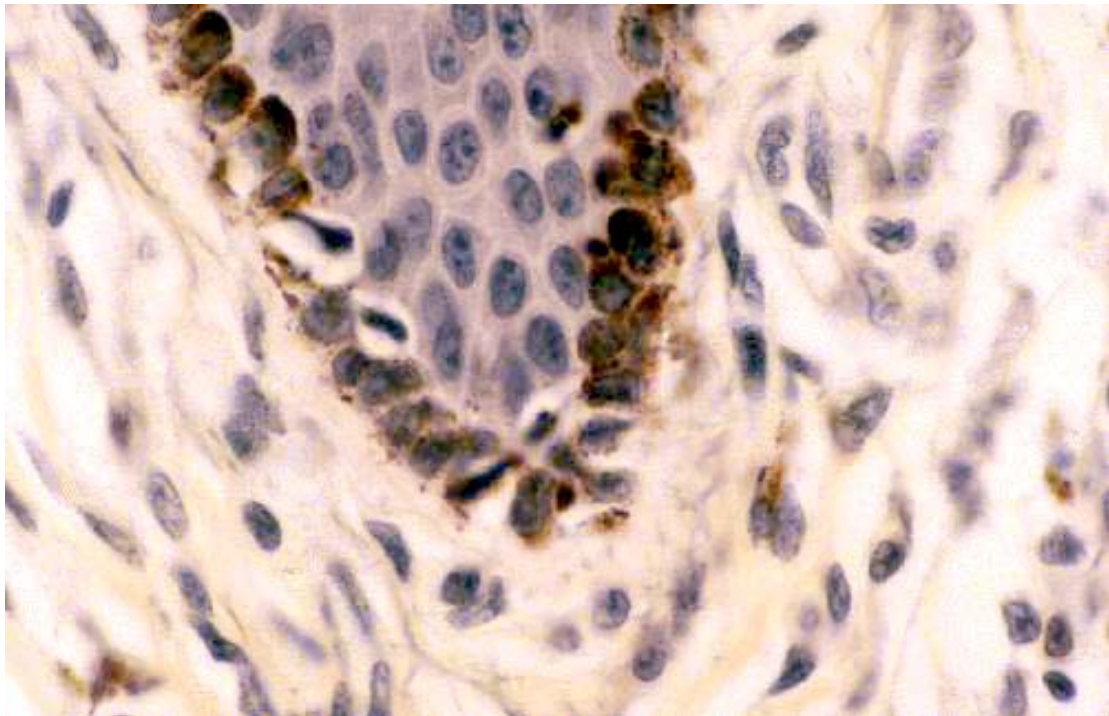


Figure 5: Fine structure of an epidermal melanocyte after immediate tanning reaction (Jimbow *et al.*, 1976).

1.1.6 Tyrosinase

Tyrosinase (monophenol monooxygenase) (EC 1.14.18.1) is an enzyme that catalyses the oxidation of phenols (such as tyrosine) and is widespread in plants and animals. Tyrosinase is a copper-containing enzyme that catalyzes the production of melanin and other pigments from tyrosine by oxidation, as in the blackening of a peeled or sliced potato exposed to air.

1.1.6.1 Chemical reaction

Tyrosinase carries out the oxidation of phenols such as tyrosine and catechol using dioxygen (O_2). In the presence of catechol, benzoquinone is formed (see reaction below). Hydrogen's removed from catechol combine with oxygen to form water (Lee & Kim, 1995).

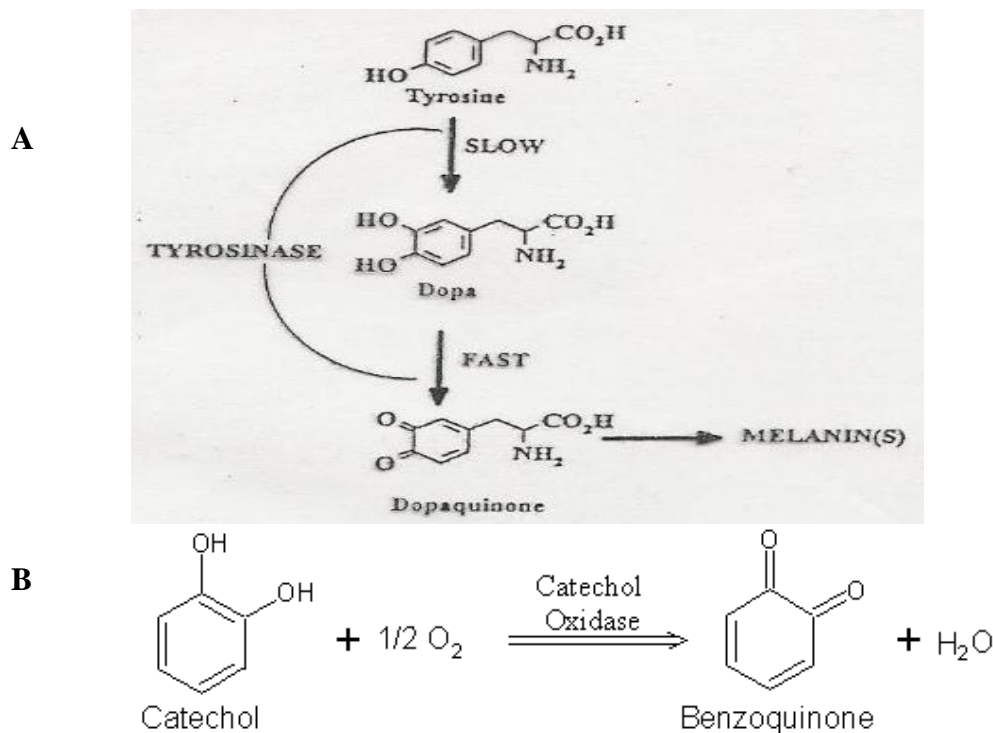


Figure 6: (A) Conversion of tyrosine to melanin(s),

(B) Conversion of catechol to benzoquinone

(Lee & Kim, 1995)

1.1.6.2 Tyrosinase structure

Tyrosinases have been isolated and studied from a wide variety of plant, animal and fungi species. Tyrosinases from different species are diverse in terms of their structural properties, tissue distribution and cellular location (Mayer, 2006). It has been suggested that there is no common tyrosinase protein structure occurring across all species (Jaenicke & Decker, 2003). The enzymes found in plant, animal and fungi tissue frequently differ with respect to their primary structure, size, glycosylation pattern and activation characteristics. However, all tyrosinases have in common a binuclear type 3 copper centre within their active site. In mushroom tyrosinase two copper atoms are each coordinated with three histidine residues

1.1.6.3 Transmembrane protein and sorting

Human tyrosinase is a single membrane spanning transmembrane protein (Kwon *et al.*, 1987). In humans, tyrosinase is sorted into melanosomes (melanosome is the organelle containing melanin) (Theos *et al.*, 2005) and the catalytically active domain of the protein resides within melanosomes. Only a small enzymatically non-essential part of the protein extends into the cytoplasm.

1.1.6.4 Active site

A model below (Figure 7, A, B, C and D) are formatted from the protein data bank file 1WX3. This file contains the coordinates for the crystal structure of a *Streptomyces* derived tyrosinase in complex with a so called "caddie protein" (Matoba & Kumagi, 2006). In all models only the tyrosinase molecule is shown, copper atoms are shown in green and the molecular surface is shown in red. In models D and E histidine amino acids are shown as a blue line representation. From model E it can be clearly seen that each copper atom within the active site is indeed complexed with three histidine residues, forming a type 3 copper center. It can also be seen from

models C and D that the active site for this protein sits within a pocket formed on the molecular surface of the molecule.

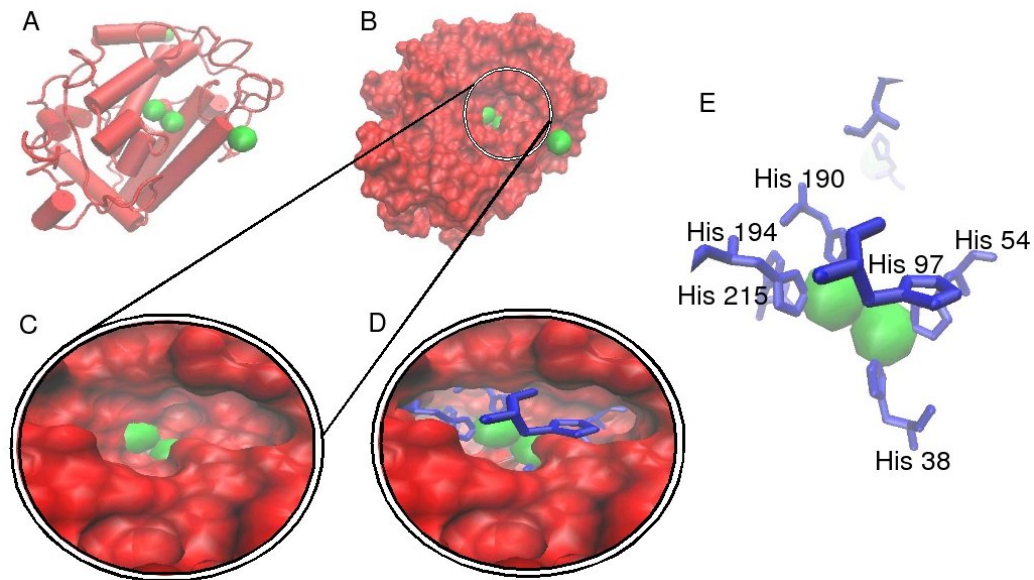


Figure 7: Crystal structure of a *Streptomyces* derived tyrosinase in complex with a so called "caddie protein" (Matoba & Kumagi, 2006).

The two copper atoms within the active site of tyrosinase enzymes interact with dioxygen to form a highly reactive chemical intermediate that then oxidizes the substrate. The activity of tyrosinase is similar to catechol oxidase, a related class of copper oxidase. Tyrosinases and catechol oxidases are collectively termed polyphenol oxidases (Matoba & Kumagi, 2006).

1.1.7 Skin colour

Skin colour varies depending on racial background, season of the year and sex. Even a single individual doesn't exhibit the same colour on all parts of the body. While skin thickness, hemoglobin and minor pigments like carotenoids affect perceived colour, the amount of melanin produced by the melanocytes primarily determines skin colour (Masuda *et al.*, 1996). Any visible pigmentary changes, whether hyper-, hypo- or depigmentation, is a cause for concern, leading to a visit to a dermatologist.

Pigmentary disturbances include epidermal hypopigmentation (leucoderma), and epidermal hyperpigmentation (melanoderma) (Bran & Maibach, 1994). Hyperpigmentary diseases, especially when occurring in the head and the neck, frequently result in loss of confidence and self esteem. In addition, maintaining a uniform basal skin tone is an important global concern. Therefore the development of an effective, controllable, and safe agent to regulate melanin synthesis in the skin is required.

1.1.7.1 Skin depigmenting agents

Defined as preparations that can suppress or inhibit melanogenesis. Due to the number and variety of maturation steps involved in melanogenesis, pigmentary regulation can be controlled at various levels. Main strategies employed to reverse hyperpigmentation and/or induce hypopigmentation include:

A. Suppress the formation of tyrosinase: Only a few ingredients are currently known to have tyrosinase formation suppression abilities. The best known active agent is natural L (+) lactic acid and its lactate salt. At higher concentrations (> 5% equivalent lactic acid), good skin lightening properties have been reported.

B. Inhibit the activity of tyrosinase: Skin lightening ingredients that can inhibit the activity of tyrosinase are widely used. Their mechanism is based on an alteration of the active center of the enzyme tyrosinase, thus reducing its activity. In most cases the ingredients are extracted from natural sources, such as bearberry (arbutin) leaves, licorice root (glycyrrhizinic acid), citrus fruits (ascorbic acid) and fermented carbohydrates (kojic acid, and gamma-pyrone compound). The tyrosinase inhibitors mentioned basically are all reductants and utilize their reducing power.

C. Directly reduce melanin: The most known active ingredient based on this mechanism is hydroquinone. Hydroquinone is still one of the most popular ingredients used in some countries. It induces skin lightening via its bleaching effect (denaturation and death of pigment cell). It has been reported to cause serious side effects if applied over longer periods of time or used in high concentrations. For that reason hydroquinone is banned for use in cosmetic products in most of the countries and/or permitted only at limited concentrations up to 2% in cosmetic formulations (Mosher *et al.*, 1987; Briganti *et al.*, 2003).

Figure 8 shows the three mechanisms of skin lightening action.

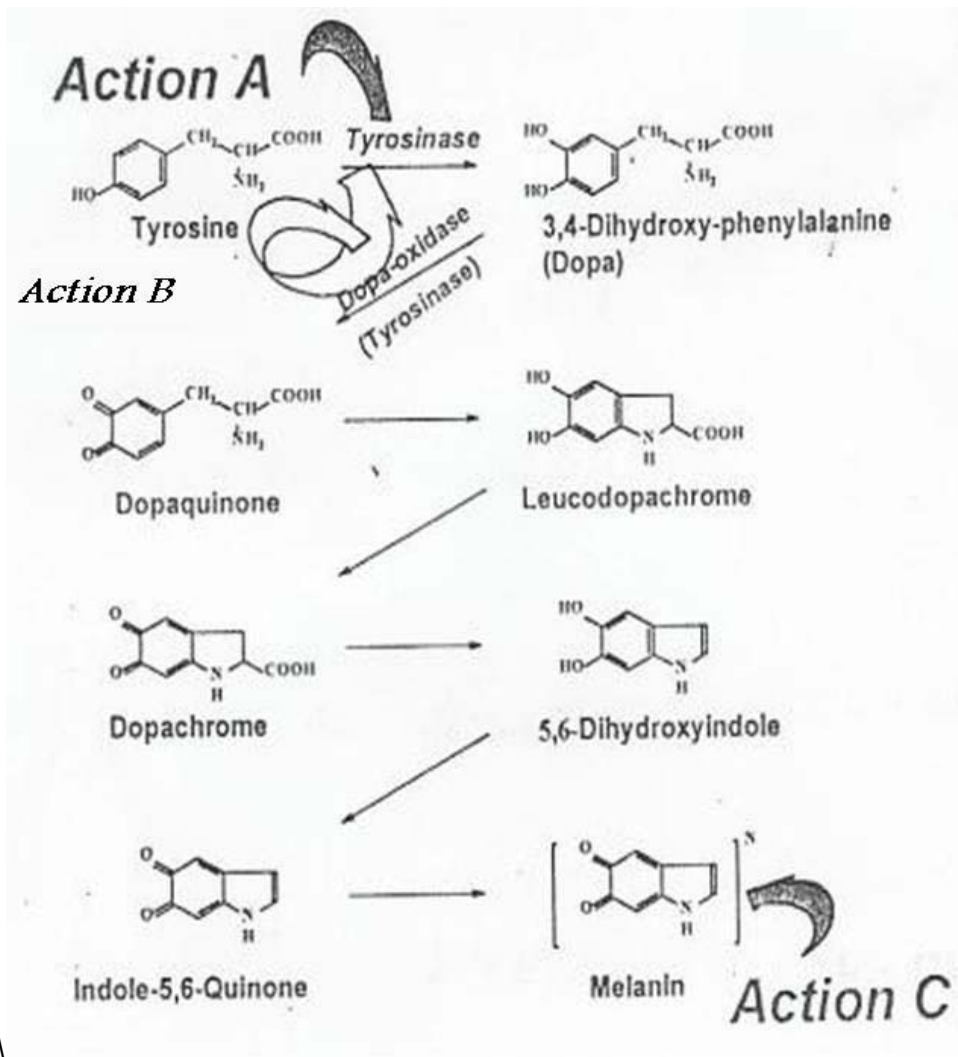


Figure 8: The mechanism of skin-depigmenting action

(Briganti *et al.*, 2003)

The most popular skin depigmenting products sold today act by inhibiting tyrosinase activity (e.g. kojic acid and arbutin). Figure 9 shows the chemical structures of these inhibitors:

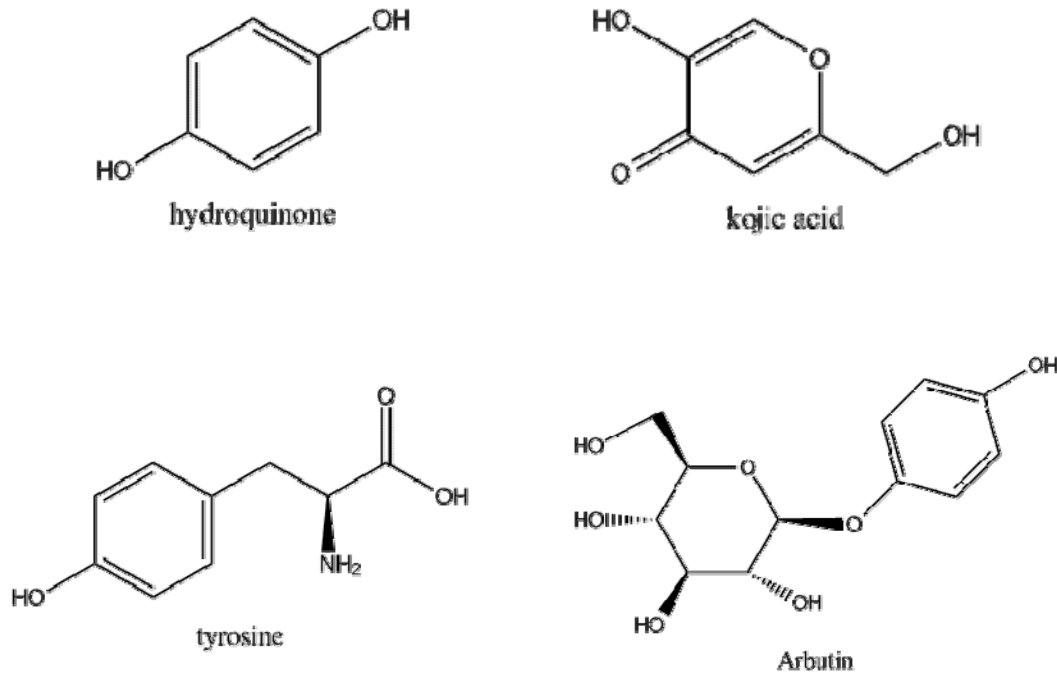


Figure 9: Chemical structure of hydroquinone, kojic acid, tyrosine and arbutin

Hydroquinone (HQ) also known as benzene-1,4-diol or quinol, is an aromatic organic compound which is a type of phenol, having the chemical formula $C_6H_4(OH)_2$ (Figure 9). Hydroquinone has been considered as a reference standard in evaluating depigmenting agents (Palumbom *et al.*, 1991, Curto *et al.*, 1999, Briganti *et al.*, 2003). It is toxic and capable of disrupting fundamental cellular processes. Reactive quinines from spontaneous oxidation of hydroquinone indiscriminately bind and damage membrane lipids and proteins, including tyrosinase. As a consequence, melanocytes are selectively destroyed resulting in permanent skin lightening (Passi & Nazzaro-Porro, 1981, Penney *et al.*, 1984, Palumbo *et al.*, 1992, Briganti *et al.*, 2003). Hydroquinone can also be very irritating resulting in irritative dermatitis, contact

dermatitis, post inflammatory pigmentation, nail bleaching and exogenous ochronosis (Pérez-Bernal *et al.*, 2000). Hydroquinone is banned for use in cosmetic products in most of the countries and/or permitted only at limited concentrations in cosmetic formulations (Ferioli *et al.*, 2001).

Kojic acid

Kojic acid ($C_6H_6O_4$; 5-hydroxy-2-(hydroxymethyl)-4-pyrone) (Figure 9) is a chelation agent produced by several species of fungi, especially *Aspergillus oryzae*, which has the Japanese common name *koji*. It has been reported as being an effective inhibitor of tyrosinase, by chelating its vital copper ion and suppressing the tautomerization from dopachrome to 5, 6- dihydroxyindole-2-carboxylic acid (Masuda *et al.*, 1996). Kojic acid up to a concentration of 1% was allowed in 1988 by Japanese regulations for use in skin care products without doctor's prescription (Nakagawa *et al.*, 1995). Kojic acid efficacy as a therapy for hyperpigmentation has been demonstrated both *in vitro* (Hira *et al.*, 1982. Ohyama & Mishima, 1990) and in clinical trials (Lim, 1999; Garcia & Fulton, 1996).

Arbutin: Arbutin (Figure 9) is glycosylated hydroquinone (β-D-glucopyranoside derivative of hydroquinone, i.e. its molecule consists of hydroquinone connected to glucose. It is believed to work by slowly releasing hydroquinone through hydrolysis, which, in turn, suppresses melanin synthesis by inhibiting the enzyme tyrosinase. Arbutin appears to have fewer side effects than hydroquinone at similar concentrations - presumably due to the more gradual release. The range of arbutin concentrations reported in the literature is 3-7% (Maeda & Fukuda, 1996; Nehei & Kubo, 2003; Hobri *et al.*, 2004) Arbutin clearly has some pigmentation reducing effect. Yet, it remains unclear how well it stacks up against hydroquinone and what

the equivalent concentrations (in terms of effectiveness) of these two agents might be. Arbutin appears to be gentler than hydroquinone as far as typical side effects like skin irritation are concerned. However, it is unclear whether the concerns recently raised regarding hydroquinone (risk of ochronosis and possible cancer risk) may apply to arbutin as well (Chakraborty et al., 1998, Maeda & Fukuda, 1996).

In conclusion, the limitations of the current depigmenting agents are either safety or effectiveness. Therefore, there is a need to find new skin depigmenting agents with more efficacy than kojic acid or arbutin and less cytotoxic than hydroquinone. The recent interest in tyrosinase in medicine, cosmetics, and food industry prompted efforts to search for new effective and safe tyrosinase inhibitors from natural and synthetic sources as a result of the key role of tyrosinase in melanin synthesis.

1.8. Drug design and discovery by pharmacophore modeling

Molecular targeting in pharmaceutical research and development requires efficient discovery, screening, detailed understanding of ADME (absorption, distribution, metabolism and excretion) processes and careful toxicological testing (Kurogi & Guner, 2001). The design of pharmaceutical agents is an extremely complex and still not completely understood process. Computational methods are now routinely employed to accelerate the lead discovery process. Computational chemistry combine the knowledge of molecular interactions and drugs activity, together with visualization techniques, detailed energy calculations, geometric considerations, and data filtered out of huge databases, in an effort to narrow down the research for potent drugs. Computer-aided drug design is a significant component of rational drug design, and is becoming more relevant as the understanding of molecular activity improves

and the amount of available experimental data that requires processing increases. Pharmacophore modeling and the three dimensional (3D) database searching are among the successful tools utilized in computer aided drug discovery. Pharmacophore model can be defined as the spatial arrangement of atoms or molecular fragments, assumed to be recognized by and to interact with a receptor or the active site of a receptor, thought to be responsible for the activity (Cohen, 1996). The concept of pharmacophore was initiated by Paul Ehrlich during his studies on the diphtheria toxin, when he introduced the concept of “Haptophoric” groups, and defined them as part of toxin molecule responsible for attachment to the cell leading to toxic effect. He was the first to coin the term “Pharmacophore”, and to use it to describe the groups of drug molecule that are essential for imparting biological activity (Ariens, 1966). However, later studies suggested that the term pharmacophore, as described by Paul Ehrlich, was insufficient in explaining the biological activity, and that a particular molecule must have certain three-dimensional (3D) geometry for recognition and binding to the intended biological receptor (Kaufman & Kerman, 1974). These advances in the pharmacophore concept were concomitant with the advances in drug receptor interaction theories, interaction forces, binding energy, and emergence of protein crystallization technique. In order to have visual insight into molecular structure and bioactivity, several computer graphical programs were developed to aid this process. These efforts started by a program developed in Princeton University during the early 1970s based on pharmacophoric pattern recognition (Gund, 1977, and Gund *et al.*, 1974). Nevertheless, the pharmacophores that were generated by this program did not enable the user to perform computerized searches, a problem that was solved later using the technique of distance geometry (Crippon, 1977).

The great advances in computational methods and computer graphics led to the development of several commercial software intended for pharmacophore modeling. Among the leader companies in this field are: MDL information systems, Oxford Molecular Group, Tripos incorporation, and Accelrys (used to be known as "Molecular Simulations Incorporation").

1.9 Pharmacophore Modeling Utilizing Catalyst® Software Package

Catalyst® software package (available from Accelrys) is one of the products for automated pharmacophore modeling and 3D database searching. These 3D searches could identify structurally novel analogues that might exhibit the biological activity of the prototype (Kaminski *et al.*, 1997).

1.9.1 Catalyst® modules

Catalyst has the following modules:

- **Catalyst/VISUALIZER** provides an easy-to-use modeling, 3D query editing, and structural editing and search environment.
- **Catalyst/COMPARE** provides the ability to compare and fit hypotheses onto molecules.
- **Catalyst/SHAPE** takes a specified 3D conformation and identifies compounds that possess similar 3D geometry. Catalyst/SHAPE complements the powerful pharmacophore and hypothesis-based searching also available within Catalyst.
- **Catalyst/ConFirm** Catalyst's ConFirm module is a conformation generation program that calculates coverage-based conformational models, thereby allowing the handling of molecular flexibility.

1.9.2 Catalyst functions

Catalyst has the following complementary capabilities:

1.9.2.1 The generation of multiple conformations

The primary aim of ConFirm's approach to conformation generation is comprehensive coverage of the low-energy conformational space using the polling algorithm (Smellie *et al.*, 1995). ConFirm examines all conformations, choosing those that are the most diverse, while keeping the molecular energy below a user-specified threshold. ConFirm supports two methods of conformation generation termed "Best" and 'Fast'. Best is more thorough in exploring conformational space, whereas "Fast" is more approximate and requires orders of magnitude less time.

1.9.2.2 Pharmacophore hypotheses automated generation

These hypotheses can be used as queries to search 3D databases to retrieve structures that fit the hypothesis, or as models to predict the activities of novel compounds. Also they help in concentrating experimentation on likely active compounds thereby accelerating the drug discovery process. Two algorithms are utilized for hypothesis-generation within Catalyst, HypoGen and HipHop.

1.9.2.3 HypoGen and HipHop

Hypogen module uses the input data (i.e., training set, conformational models, chemical features, parameters, etc.) to generate the ten top scoring hypothesis models that best correlate estimated activities with measured activities. The estimated activities are computed using regression information obtained from a simple regression of geometric fit values versus activity of the training set members. The greater the geometric fit value, the more active the compound. The geometric fit is

based on two factors: 1) the feature weight and 2) how well the chemical features of the pharmacophore overlap with the subject molecule. HipHop module provides feature-based alignment of a collection of compounds without considering activity. HipHop matches the chemical features of a molecule, against drug candidate molecules or searches of 3D databases. The resulting hypotheses can be used to iteratively search chemical databases to find new lead candidates.

1.9.2.4 Three-dimensional database searching

Pharmacophore hypotheses generated by HipHop or HypoGen could be used as a query to search Catalyst databases for compounds with similar activities and thereby broaden the knowledge of the structure-activity relationships of any particular target. Furthermore, Catalyst[®]/SHAPE module can be utilized for searching 3D corporate or project databases, or combinatorial libraries for shape similarity between molecules (Hahn, 1997).

1.9.2.5 Database Searching using CATALYST/Shape[®] Program

Efforts have been made regarding the steric environment of molecules fulfilling the search query, since there is no guaranty that the trapped molecule size will fit the binding site correctly, and it will not be hindered by size of the binding site.

CATALYST can deal with such case by its build in program termed as CATALYST/Shape[®], where the most active molecule is mapped on then a surface can be generated over the molecule to define an allowed region. This surface could be

merged with the original search query to generate new refined one used later as more accredited search query.

This work includes pharmacophore modeling of tyrosinase inhibitors utilizing HipHop module. The best pharmacophore was subsequently used as 3D search query to screen minbiobyte and Medeterian normal flora Databases for new Tyrosinase inhibitors. The resulting hits were filtered according to Lipinski's rule of five, some hits were chosen for subsequent in vitro testing for tyrosinase inhibition.

1.10 Objectives

- Construction of high quality pharmacophore model for the enzyme tyrosinase.
- In-silico* screening for new tyrosinase inhibitors.
- In-vitro* screening for new tyrosinase inhibitors.

2. Experimental

2.1. Molecular Modeling

2.1.1 Software and Hardware

The following software packages were utilized in the present research.

- CATALYST (Version 4.11), Accelrys Inc. (www.accelrys.com), USA.
- CERIOUS2 (Version 4.10), Accelrys Inc. www.accelrys.com, USA.
- CS ChemDraw Ultra 7.01, Cambridge Soft Corp. (<http://www.cambridgesoft.com>), USA.

Pharmacophore and QSAR modeling studies were performed using CATALYST® (HYPOGEN module) and CERIOUS2 software suites program from Accelrys Inc. (San Diego, California, www.accelrys.com) installed on a Silicon Graphics Octane2 desktop workstation equipped with a 600 MHz MIPS R14000 processor (1.0 GB RAM) running the Irix 6.5 operating system. Structure drawings were performed employing CS ChemDraw Ultra 7.01 installed on Pentium 4 PC.

2.1.2. Data mining

The structures of 7 diverse tyrosinase inhibitors were collected carefully from published literature (Hoi-Seon, 2002; Kyoko Ishiguro & Isao Kubo, 1999); only non-competitive inhibitors were included in modeling. The *in vitro* bioactivities of the collected inhibitors are expressed as the concentration of the test compound that inhibited mushroom tyrosinase by 50% (IC₅₀). Figure 10 shows the collected inhibitors and their IC₅₀ values.

2.1.3 Molecular modeling

The two-dimensional (2D) chemical structures of the inhibitors were sketched using ChemDraw Ultra and saved in MDL-mol file format. Subsequently, they were imported into Discovery Studio, converted into corresponding standard 3D structures.

The resulting 3D structures were utilized as starting conformers for CATALYST conformational analysis

2.1.3.1. Conformational analysis.

Molecular flexibility was taken into account by considering each compound as a collection of conformers representing different areas of the conformational space accessible to the molecule within a given energy range. Accordingly, the conformational space of each inhibitor was explored adopting the “best conformer generation” option within CATALYST based on the generalized CHARMM force field implemented in the program. Default parameters were employed in the conformation generation procedure, i.e., conformational ensembles was generated with an energy threshold of 20 kcal/mol from the local minimized structure and a maximum limit of 250 conformers per molecule. Hence, this search procedure will probably identify the best 3D arrangement of chemical functionalities explaining the activity variations among the training set (Clement *et al.*, 2000; Accelrys Software Inc., San Diego, 2005).

2.1.3.2. Pharmacophore modeling.

HipHopRefine identifies 3D spatial arrangements of chemical features that are common to active molecules in a training set. These configurations are identified by a pruned exhaustive search, starting from small sets of features and extending them until no larger common configuration is found. Active training set members are evaluated on the basis of the types of chemical features they contain, along with the ability to adopt a conformation that allows those features to be superimposed on a particular configuration. The user defines how many molecules must map completely

or partially to the hypothesis via the Principal and MaxOmitFeat parameters. These options allow broader and more diverse hypotheses to be generated.

The resultant pharmacophores are ranked as they are built. The ranking is a measure of how well the active training molecules map onto the proposed pharmacophores, as well as the rarity of the pharmacophore model. If a particular pharmacophore is “rare” then it will be less likely to map to an inactive compound and therefore it will be given a higher rank (Clement *et al.*, 2000; Accelrys Software Inc., San Diego, 2005).

HipHopRefine uses inactive training compounds to construct excluded volumes that resemble the steric constraints of the binding pocket. It identifies spaces occupied by the conformations of inactive compounds and free from the active inhibitors. These regions are then filled with excluded volumes. HipHopRefine returns by default a maximum of 10 high-ranking pharmacophores from each automatic run (Catalyst User Guide, Accelrys Software Inc., San Diego, 2005, 9th European CATALYST User Group Meeting, San Diego, CA, 2006).

The 7 training compounds were fed into HipHopRefine, and the software was instructed to explore up to four-featured pharmacophoric space of the following possible features: hydrogen bond acceptor (HBA), hydrogen bond donor (HBD), hydrophobic and hydrophilic. The number of features of any particular type was allowed to vary from 0 to 3. We defined IC₅₀ value of 1.0 mM as the activity/inactivity cutoff. Accordingly, inhibitors of IC₅₀ values ≤ 1 mM were regarded as “actives” and were assigned Principal and MaxOmitFeat values of 2 and 0, respectively, to ensure that all of their chemical features will be considered in building the pharmacophore space (Catalyst User Guide, Accelrys Software Inc., San Diego,

2005, 9th European CATALYST User Group Meeting, San Diego, CA, 2006). However, compound 2 (Table 1) was assigned Principal and MaxOmitFeat values of 1 and 2, respectively to account for the fact that it exhibited borderline bioactivity (0.97 mM). On the other hand, the inhibitor of $IC_{50} > 1$ mM (compound 1 in Figure 10) was considered inactive and was assigned a Principal value of zero (Catalyst User Guide, Accelrys Software Inc., San Diego, 2005, 9th European CATALYST User Group Meeting, San Diego, CA, 2006).

Spaces occupied by conformers and/or mappings of this compound and free from conformers and/or mappings of active compounds are filled with excluded volumes. HipHop-REFINE was configured to allow a maximum of 100 exclusion spheres to be added to the generated pharmacophoric hypotheses. This represents the default value for the number of excluded volumes in HipHop-REFINE. Table 1 shows the training compounds and their corresponding Principal and MaxOmitFeat parameters.

The followings are important HipHopRefine control parameters used for hypotheses generation (HipHop User Guide Version 3.1, Catalyst 4.10, Accelrys Inc., San Diego, CA, 2005. (http://www.accelrys.com/doc/life/catalyst410/help/hipHop/HipHop_23TOC.doc.htm)).

- Spacing: This parameter controls the minimum allowed inter-feature distance in the resulting hypotheses. The value was set to 2.0 Å.
- MinPoints: The default value of this parameter is 4, specifying a minimum of four individual feature components for a generated hypothesis.
- MinSubset Points: Only configurations of features in input molecules, with at least the number of points specified by this option, are considered when identifying a candidate hypothesis. The default value is 4.

- Superposition error, check superposition and tolerance factor: The three control parameters together check the superposition of compounds for hypothesis generation. All three have a default value of 1. Reducing the value from its default tightens the fit.
- Misses: This value specifies the number of compounds in the training set that do not have to map to all features in generated hypotheses. This value was modified from the default of 1 to 2.
- Feature misses: This specifies the number of compounds allowed not to map any particular feature in a generated hypothesis. The default value is 1.
- Complete misses: This option specifies the number of molecules in the training set that do not have to map to more than one feature per generated hypothesis. In current case the default value (zero) was employed.
- Mapping coefficient: This parameter controls the importance of having compounds with similar structure map to a hypothesis in a similar way. Increasing this parameter will penalize the hypotheses that deviate from this behavior. The default value is 0.

2.1.4 *In silico* screening for new tyrosinase Inhibitors.

The highest ranking model, Hypo 1 (Table 2, Figure 11), was employed as 3D search query against an *in house* built database of natural products isolated from East Mediterranean flora (Lee *et al.*, 1997, Bartram, 1995; Bown, 1995 and Dothan, 1978) and Minbiobyte structural database provided with Catalyst (1901 compounds) using the “Best Flexible Database Search” option within CATALYST. It captured 489 compounds. The hits were subsequently fitted against Hypo1 using Fast Fit approach of CATALYST, and the lowest 350 hits (of fit values equal or near to zero) were

excluded. The remaining hits (139 compounds) were evaluated according to Lipinski's rule of five (Lipinski, 2004). However, hits of a maximum of one Lipinski's violation were retained for subsequent processing. To further enhance the drug-likeness of the remaining hits (90 compounds), we excluded compounds of molecular weights higher than 450 Da. Table 3 shows minibiobyte Hits and table 4 shows the Flora Hits.

2.2 *In vitro* experimental studies:

2.2.1. Chemicals, Materials and Equipments

Mushroom tyrosinase, L-tyrosine, kojic acid, arbutin and 3,4-(Methylenedioxy) cinnamic acid were all purchased from Sigma Chemical Co (Sigma, Germany), other chemicals were purchased from the Aldrich Chemical Co. (Wisconsin, U.S.A.).

The equipment used included rotavapor, R110 (Büchi, Switzerland) with bath temperature 40-50°C, a cooler circulator (Julabo, Germany), microplate reader (BIO-TEK, KC junior), vortex mixer (Vision Scientific, LTD, Korea), pH meter (Cambridge, U.K.), and 96-well microplate (Nunc, Denmark). All glasswares were rinsed thoroughly using soap and deionized water then washed with acetone and dried in oven (100-130°C) over night.

2.2.2 Plant Materials:

Fresh plant *Annona cherimola* Mill. (Annoaceae) was purchased from the local Jordanian market. Taxonomic identity of the plant was confirmed in comparison with the specimen at the Herbarium, Faculty of Science, University of Jordan, and using descriptive references (Dothan, 1978).

2.2.3 Preparation of plant extracts:

Fresh plant material (1.0 kg) were cut into small pieces and extracted twice with 80% methanol (2L) at room temperature and filtered. The combined filtrate was concentrated to dryness at 45°C in a vacuum rotatory evaporator (Büchi, Switzerland). The dried extract was used for biological screening of tyrosinase inhibitory activities.

2.3 Anti-tyrosinase activity

2.3.1 Principle

Tyrosinase inhibition assay was performed with kojic acid & arbutin as standard inhibitors for the enzyme tyrosinase in a 96-well microplate format using microplate reader (BIO-TEK, KC junior), according to the method developed by (Vanni *et al.* 1990, Lee *et al.*, 1997).

This method is based on measuring the ability of each inhibitor at different concentrations to inhibit mushroom tyrosinase ability to convert L-tyrosine to L-dihydroxyphenylalanine (L-DOPA).

As the activity of the enzyme on its substrate increases, the absorbance of L-DOPA will increase, accordingly, as the inhibitor activity increases, the absorbance of L-DOPA will decrease. The reaction will be completed within virtually 20 minutes. The absorbance of the colored reaction have specific $\lambda_{max} = 475\text{nm}$.

The inhibitory activity against enzymatic oxidation of L-tyrosine was calculated by the following equation:

Inhibitory percentage = $[(A_{475\text{control}} - A_{475\text{sample}}) / A_{475\text{control}}] \times 100\%$ (Vanni *et al.*, 1990, Lee *et al.*, 1997).

Where A_{475} sample and A_{475} control were the absorbance values in the presence and absence of inhibitor respectively; each absorbance value was recorded against the corresponding reference blank (in phosphate buffer alone).

The IC_{50} (the concentration required by each inhibitor to inhibit the activity of 50% of the enzyme) was determined in order to compare the efficiency of *Annona cherimola* Mill plant extract and 3,4-(Methylenedioxy) cinnamic acid with the inhibitory activity of the standards.

2.3.2 Inhibitor standards

The inhibitor standards used involved kojic acid & arbutin. These substances possess anti-tyrosinase activity and they are widely used as standard materials to evaluate the *in vitro* activities of test materials with anti-tyrosinase activity. In this experiment, IC_{50} of the standard is compared with IC_{50} of *Annona cherimola* Mill plant extract and 3,4-(Methylenedioxy) cinnamic acid. These standard inhibitors are incorporated in many commercial formulations as skin lightening products.

2.3.3 Procedure for measurements of inhibitory activity against tyrosinase-catalysed oxidation of L-tyrosine.

Tyrosinase activity, using L-tyrosine as the substrate, was assayed spectrophotometrically as described by (Vanni *et al.* 1990, Lee *et al.*, 1997). A (80 μ l) of different concentrations of *Annona cherimola* Mill plant extract and 3,4-(Methylenedioxy) cinnamic acid dissolved in potassium phosphate buffer, pH 6.5 were added to an assay mixture containing (80 μ l) of 0.1 mg/ml of L-tyrosine solution, (70 μ l) 50 mM potassium phosphate buffer, pH 6.5 and 20 μ l (16 units) of mushroom tyrosinase (prepared in potassium phosphate buffer, pH 6.5) in a 96-well microplate (Nunc, Denmark), with a total volume of 250 μ l. The assay mixture was

incubated for 10 min at 37 C°. After incubation, the absorption at 475 nm (OD₄₇₅) was determined in a microplate reader (KC junior). Kojic acid, and arbutin were used as positive controls and were examined at five different concentrations (5, 10, 50, 75 and 100 µg/ml). 3,4-(Methylenedioxy) cinnamic acid was selected as a hit compound for our model and was tested at five concentrations (5, 10, 50, 75 and 100 µg/ml). From the flora hits *Annona cherimola* Mill plant extract was selected and examined at five different concentrations (50, 100, 250, 500 and 1000 µg/ml). All measurements were carried out in triplicate. The IC₅₀ was determined for *Annona cherimola* Mill plant extract, 3,4-(Methylenedioxy) cinnamic acid, Kojic acid and Arbutin.

3. Results and Discussion

3.1. Data mining and conformational coverage.

The 2D structures of the 7 diverse tyrosinase inhibitors (1–7, Figure 10) were imported into CATALYST and converted automatically into plausible 3D single conformer representations via the rule-based methods implemented within CATALYST.

The conformational space of each inhibitor was extensively sampled utilizing the poling algorithm employed within the CONFIRM module of CATALYST. Poling promotes conformational variation via employing molecular mechanical force field algorithm that penalizes similar conformers (Smellie *et al.*, 1995 a&b). Conformational coverage was performed employing the “best” module to ensure extensive sampling of conformational space. Efficient conformational coverage guarantees minimum conformation-related noise during pharmacophore generation and validation stages. Pharmacophore generation and pharmacophore-based search procedures are known for their sensitivity to inadequate conformational sampling within the training compounds (Sheridan, 2002, Catalyst User Guide, Accelrys Software Inc., San Diego, 2005, Sutter, 2000)

3.2. Pharmacophore modeling

CATALYST includes two separate pharmacophore-modeling modules, namely: HypoGen and HipHop. HypoGen enables automatic pharmacophore construction by using a collection of at least 16 molecules with bioactivities spanning over four orders of magnitude (Catalyst User Guide, Accelrys Software Inc., San Diego, 2005, Sutter, 2000). On the other hand, HipHop generates common feature pharmacophores regardless to the activities of the training compounds (Catalyst User Guide, Accelrys Software Inc., San Diego, 2005, 9th European CATALYST User Group Meeting, San

Diego, CA, 2006). Still, both modules generate 3D pharmacophores that can be used as search queries to virtually screen 3D-structural libraries. However, as the bioactivity spread of inhibitors from any particular literature source is less than four logarithmic cycles, we avoided using HypoGen. Therefore, it was decided to employ HipHop to generate common feature pharmacophore(s) for tyrosinase inhibitors. Furthermore, we employed the REFINE module to incorporate excluded volumes in the resulting binding hypotheses. Excluded volumes resemble sterically inaccessible regions within the binding site (Catalyst User Guide, Accelrys Software Inc., San Diego, 2005, 9th European CATALYST User Group Meeting, San Diego, CA, 2006). All the 7 inhibitors were used as training subset for HipHop-REFINE modeling (Figure 10). Effective pharmacophore modeling requires training sets of adequate structural diversity to elucidate the common functional features responsible for ligand–receptor affinity across wide ligand diversity. HipHop-REFINE was instructed to explore up to five-featured pharmacophoric space.

The software was instructed to explore pharmacophoric models incorporating from zero to three features from any particular selected feature type (i.e., HBA, HBD, and Hydrophobic). Eventually, 10 optimal pharmacophoric hypotheses were generated. However, they all shared comparable features. Table 2 shows the pharmacophoric features of the generated models. The highest-ranking model (Hypol) is comprised of one hydrophobic area and three HBAs features and 21 excluded volumes.

(Figure 11) shows how Hypol fits three active training inhibitors. Evidently, from the figure, the hydrophobic aromatic heads of the three inhibitors (i.e., the benzothiophene of 139, the benzofuran of 71 and 122) reside deep into the proposed receptor where they interact with two hydrophobic pockets and one hydrogen-bonding site. On the other hand, the carboxylate moieties of the three compounds seem to

interact with certain positively charged residue at the outer rim of the proposed receptor.

3.4. *In silico* screening of flora and minibiobyte databases and subsequent *in vitro* evaluation

Hypol was employed as 3D search query to screen the flora and minibiobyte databases (7401 compounds). The search process took nearly 3 h and it captured 489 hits. Hits are defined as those compounds that possess chemical groups that spatially overlap (map) with corresponding features within the pharmacophoric model. The hits were subsequently fitted against Hypol and those of fit values 0 were excluded from subsequent processing. A low fit value indicates that although the chemical functions of the particular hit(s) overlap with the corresponding pharmacophoric features, the centers of the functional groups (of the hit) are displaced from the centers of the corresponding pharmacophoric features. Therefore, excluding poor fitters should improve the success rates of the retained hits. The remaining hits (139 compounds) were filtered according to Lipinski's "rule of five" to retain drug-like molecules (Lipinski, 2004). However, we allowed a maximum of one Lipinski's violation to enrich the chemical diversity of the selected hits, particularly under the limiting effects of the 92 exclusion volumes in Hypol. This selection retained 90 hit molecules. Some of the hits found by the constructed pharmacophore were already documented in literature to have tyrosinase inhibition activity such as pimelic acid (Nazzaro-Porro & Passi, 1978), methinonin (Chen & Chavin, 1978) and rhamnose (Kamya *et al.*, 1994; Nakagawa & Takahashi, 2004; Tokiwa & Raku, 2006) from minibiobyte, and *Rosa* (Choi *et al.*, 2003; Arung *et al.*, 2005), *Curcubita* (Nose & Miki, 1994; Tazawa & Warashina, 2001), *Beta vulgaris* (Weidenhagen & Heinrich, 2006; Josefa *et al.*, 2002; Pruidze & Grigorashvili, 1975) were reported from Flora database.

Three hit compounds have been selected for testing their tyrosinase inhibitory activities: L-methionine, ethyl nicotinic acid, and 3, 4-(Methylenedioxy) cinnamic acid. From flora database we have also screened three plant extracts: *Cucurbita pepo*, *Beta vulgaris* and *Annona cherimola* Mill. All these were examined at 3 different concentrations (50, 200 and 400 $\mu\text{g/ml}$) as a preliminary screening test.

Among these L-methionine and ethyl nicotinic acid showed no inhibitory activity. In addition, both *Cucurbita pepo* and *Beta vulgaris* plant extracts showed no inhibitory activity. From these preliminary data, 3,4-(Methylenedioxy) cinnamic and *Annona cherimola* Mill plant were used for further investigation.

3.2 Measurements of inhibitory activity against tyrosinase-catalysed oxidation of L-tyrosine.

Kojic acid and arbutin were used as positive controls, and were examined at five different concentrations (5, 10, 50, 75 and 100 $\mu\text{g/ml}$). 3,4-(Methylenedioxy) cinnamic acid was selected as a hit compound for our model and was tested at five concentrations (5, 10, 50, 75 and 100 $\mu\text{g/ml}$). From the flora hits *Annona cherimola* Mill plant extract was selected and examined at five different concentrations (50, 100, 250, 500 and 1000 $\mu\text{g/ml}$). All measurements were carried out in triplicate. The IC_{50} , the concentration at which half the original tyrosinase activity is inhibited, was determined for both 4-(Methylenedioxy) cinnamic acid and the plant extract.

Figure 14 represent the results of screening test for inhibitory activity of tyrosinase enzyme for kojic acid, arbutin and 3,4-(Methylenedioxy) cinnamic acid. Figure 15 represents the results of screening test for inhibitory activities of tyrosinase enzyme for *A.cherimola* plant extract. The IC_{50} for kojic acid, arbutin, and 3,4-(Methylenedioxy) cinnamic acid and *A.cherimola* plant extract was found to be as

follows: kojic acid ($IC_{50} = 6 \mu\text{g/ml}$), arbutin ($IC_{50} = 65 \mu\text{g/ml}$). 3,4-(Methylenedioxy) cinnamic acid ($IC_{50} = 60 \mu\text{g/ml}$), *A. cherimola* ($IC_{50} = 80 \mu\text{g/ml}$).

From these results it is clear that 3,4-(Methylenedioxy) cinnamic acid and *A. cherimola* plant extract were both able to inhibit tyrosinase activity *in vitro*. Our results suggest that this pharmacophore for the enzyme tyrosinase can be a useful tool for finding potential tyrosinase inhibitors.

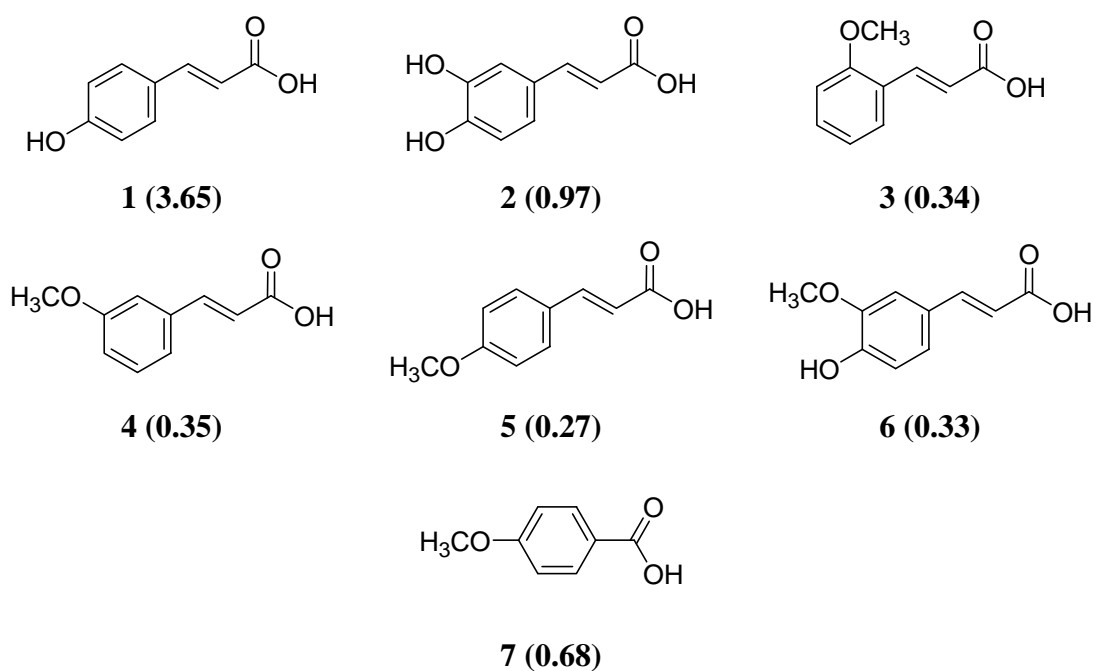
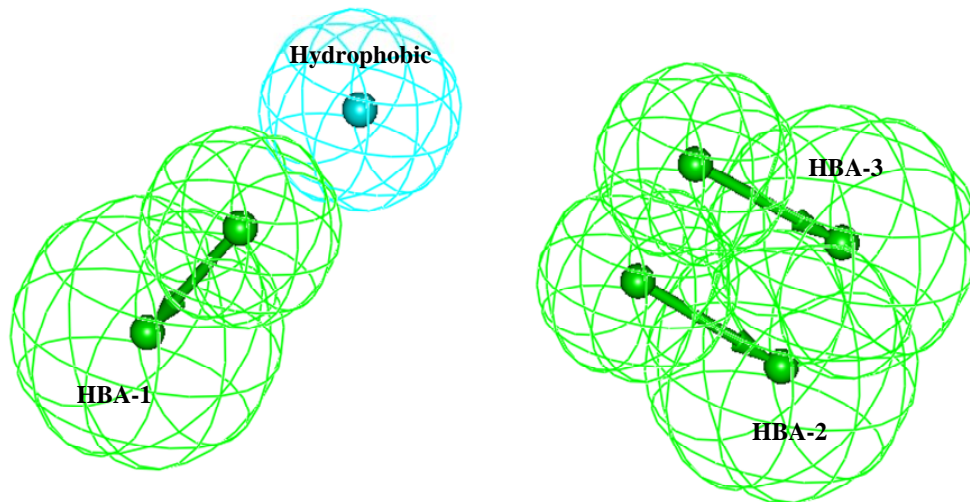


Figure 10: Chemical structures of the 7 tyrosinase inhibitors applied to HipHopRefine modeling. The activities are expressed in brackets as IC_{50} in mM

A.



B.

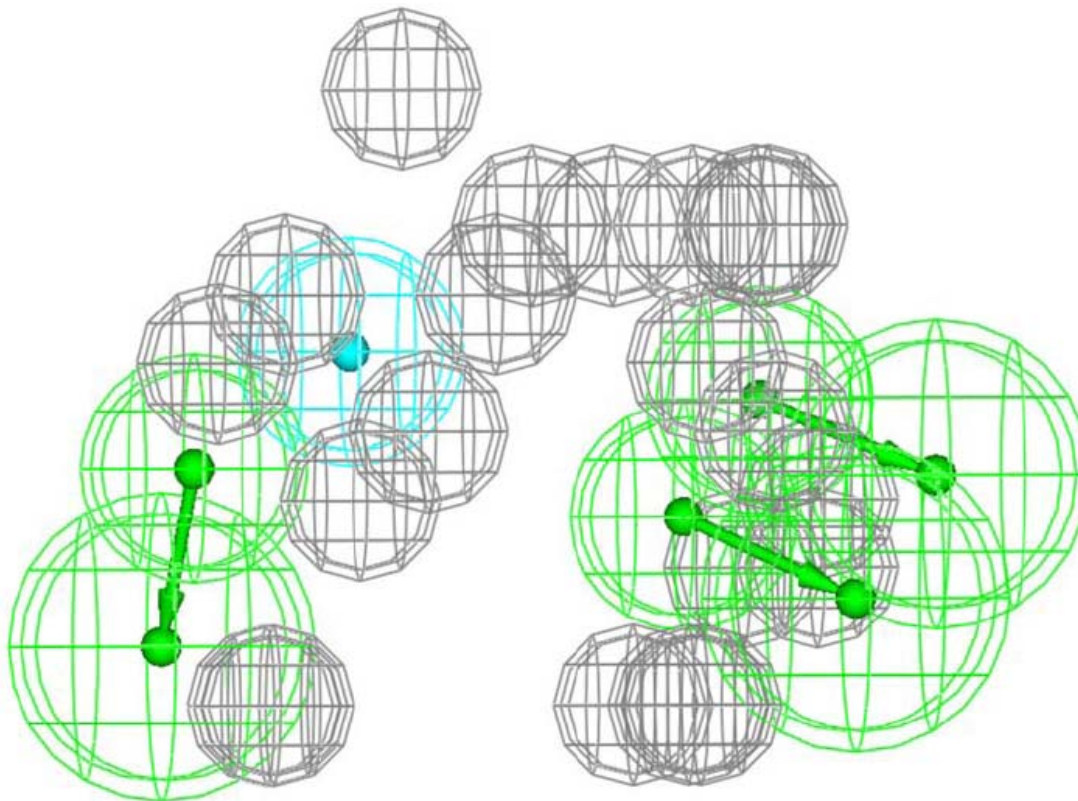


Figure 11: (A) The pharmacophoric features of Hypo 1 (HBA: hydrogen bond acceptor) (B) with added excluded volumes (gray spheres) Excluded volumes resemble sterically inaccessible regions within the binding site.

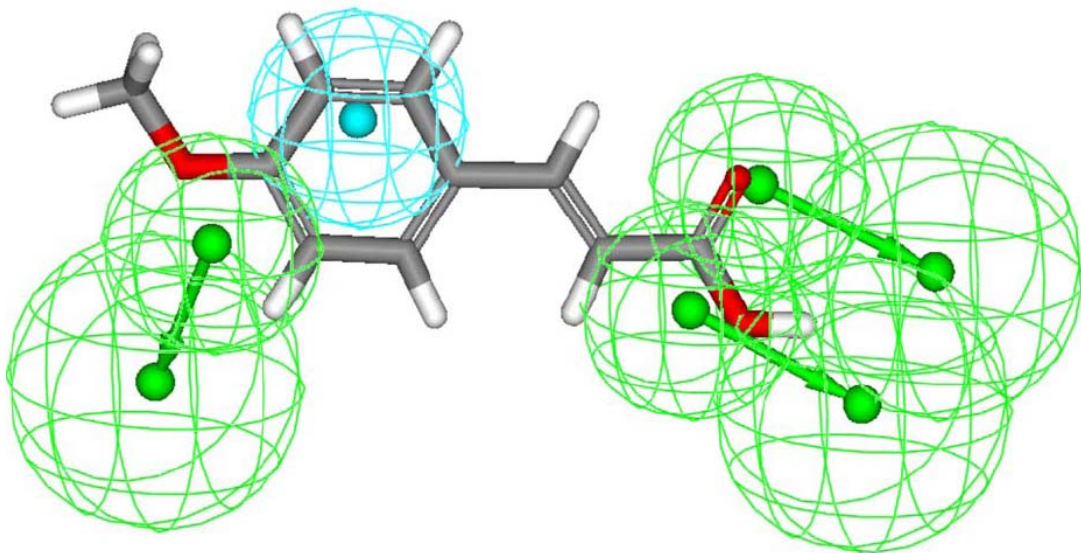
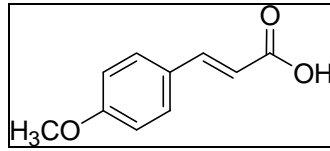


Figure 12: Mapping the highest ranking pharmacophore model against inhibitor number 5.

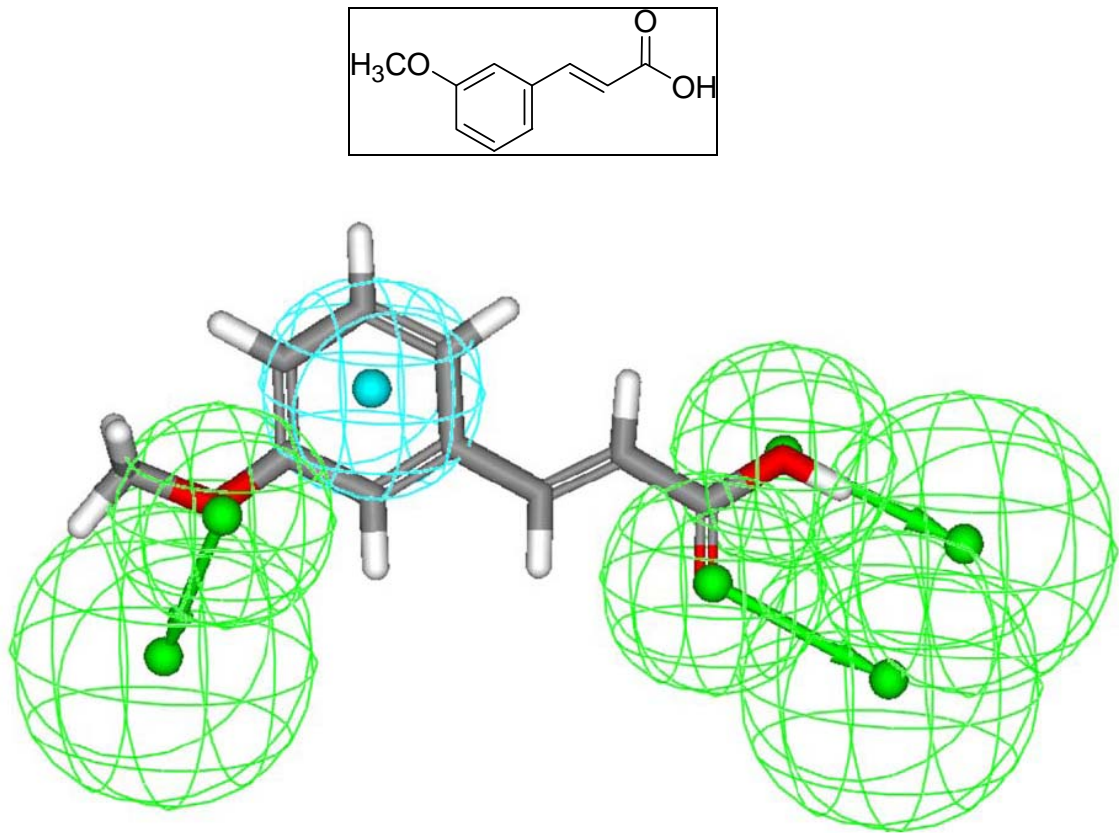
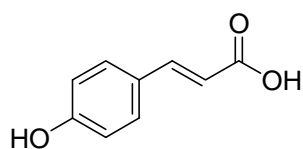


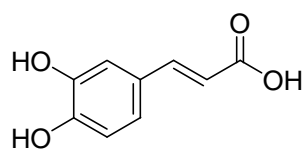
Figure 13: Mapping the highest ranking pharmacophore model against inhibitor number 4.

Table 1: The training list used for pharmacophore modeling of tyrosinase inhibitors.

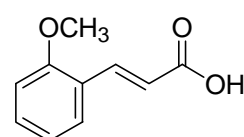
Compound ^a	Principal value	MaxOmitFeat
1	0	2
2	1	2
3	2	0
4	2	0
5	2	0
6	2	0
7	2	0

^aCompounds' numbers as below

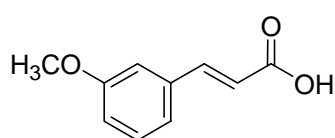
1



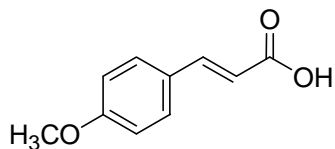
2



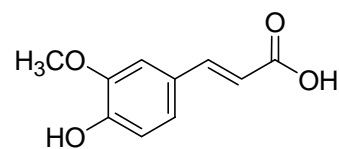
3



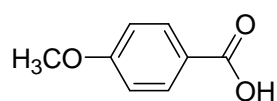
4



5



6



7

Table 2: The pharmacophoric features of the 10 hypotheses generated by the HipHopRefine automatic run.

Hypothesis	Hypothesis Rank ^a	Features	Number of Exclusion Spheres ^b
1	47.7382	3 x HBA, Hydrophobe	21
2	47.7382	3 x HBA, Hydrophobe	16
3	46.8804	3 x HBA, Hydrophobe	15
4	40.8472	2 x HBA, 2 x Hydrophobe	8
5	40.8472	2 x HBA, 2 x Hydrophobe	7
6	39.5787	2 x HBA, 2 x Hydrophobe	7
7	36.8313	2 x HBA, 2 x Hydrophobe	6
8	36.0772	3 x HBA	22
9	35.6712	3 x HBA	15
10	33.2231	2 x HBA, 2 x Hydrophobe	11

^aThis ranking is as provided in the log file of the HipHopRefine automatic run. The ranking is a measure of how well the active training molecules map onto the proposed pharmacophores, as well as the rarity of the pharmacophore models.

^bExcluded volumes resemble sterically inaccessible regions within the binding site.

Table 3: Minibiobyte Hits

Name	Mol Wt	Mol Formula
Arginine	174.202	$C_6H_{14}N_4O_2$
1,3 dicarboxylic acid cyclopentane	158.154	$C_7H_{10}O_4$
(3, 4 methylenedioxy) cinnamic acid	192.171	$C_{10}H_8O_4$
Rhamnose	164.158	$C_6H_{12}O_5$
Hydroxy-phenoxy-acetic acid	168.149	$C_8H_8O_4$
Acetyl -L-methionine	191.245	$C_7H_{13}NO_3S$
Methyl-succinic acid	132.116	$C_5H_8O_4$
Ethyl ester nicotinic acid	151.165	$C_8H_9NO_2$
Pimelic acid	160.169	$C_7H_{12}O_4$

Table 4: Flora Hits

Name	Mol Wt	Mol Formula
Beta vulgaris 27	168.149	C ₃ H ₈ O ₄
Beta vulgaris 6	166.139	C ₆ H ₆ N ₄ O ₂
Beta vulgaris 22	154.122	C ₇ H ₆ O ₄
Beta vulgaris 16	182.176	C ₉ H ₁₀ O ₄
Beta vulgaris 12	152.149	C ₈ H ₈ O ₃
Rosa chinensis 11	154.122	C ₇ H ₆ O ₄
Annona cherimola 39	168.149	C ₈ H ₈ O ₄
Annona cherimola 36	182.176	C ₉ H ₁₀ O ₄
Annona cherimola 40	168.149	C ₈ H ₈ O ₄
Rosa chinensis 14	180.16	C ₉ H ₈ O ₄
Beta vulgaris 14	138.123	C ₇ H ₆ O ₃
Beta vulgaris 17	138.123	C ₇ H ₆ O ₃
Annona cherimola 35	168.149	C ₈ H ₈ O ₄
Annona cherimola 28	182.176	C ₉ H ₁₀ O ₄
Annona cherimola 16	152.149	C ₈ H ₈ O ₃
Annona cherimola 42	166.176	C ₉ H ₁₀ O ₃
Cucurbita pepo 22	154.165	C ₈ H ₁₀ O ₃
Faba vulgaris 2	181.191	C ₉ H ₁₁ NO ₃
Annona cherimola 11	123.111	C ₆ H ₅ NO ₂
Annona cherimola 26	152.149	C ₈ H ₈ O ₃
Annona cherimola 33	194.187	C ₁₀ H ₁₀ O ₄
Lilium candidum 11	159.141	C ₆ H ₉ NO ₄
Cucurbita pepo 30	164.16	C ₉ H ₈ O ₃
Cucurbita pepo 32	166.176	C ₉ H ₁₀ O ₃
Salvia 194	198.175	C ₉ H ₁₀ O ₅
Salvia 911	197.19	C ₉ H ₁₁ NO ₄
Salvia 924	212.202	C ₁₀ H ₁₂ O ₅
Cucurbita pepo 9	168.192	C ₉ H ₁₂ O ₃

Note: The number after the plant name is the number of the compound in the flora Database

4. Conclusion

Tyrosinase enzyme has become an important target for the discovery of new tyrosinase inhibitors due to their broad applications in many fields. This work includes pharmacophore modeling of tyrosinase inhibitors utilizing HipHop-REFINE. The best binding hypothesis was subsequently used as 3D search query to screen the 3D database for new tyrosinase inhibitors. The resulting hits were filtered according to Lipinski's rule of five and evaluated using spectrophotometry enzyme assay. Some of the hits like 3,4-(Methylenedioxy) cinnamic acid and *A. cherimola* plant extract which exhibited anti-tyrosinase activity proved that the pharmacophore model presented can constitute a step forward in the search of new structural features with this activity and to discover new potent selective tyrosinase inhibitors.

5. Future work

- To isolate and identify the active compounds that exhibits tyrosinase inhibitory activities in the plant extract of *Annona cherimola* Mill.
- To study the efficiency of 3,4-(Methylenedioxy) cinnamic acid and plant extract of *Annona cherimola* Mill on the degree of skin lightening effect using *in vivo* experiments followed by toxicological studies to evaluate the possible toxicity of 3,4-(Methylenedioxy) cinnamic acid & *Annona cherimola* plant extract.
- 3D search of new databases to find new tyrosinase inhibitors using the constructed pharmacophore.

Figure 14

Percent tyrosinase inhibition

By

arbutin, 3,4-(Methylenedioxy)cinnamic acid and kojic acid

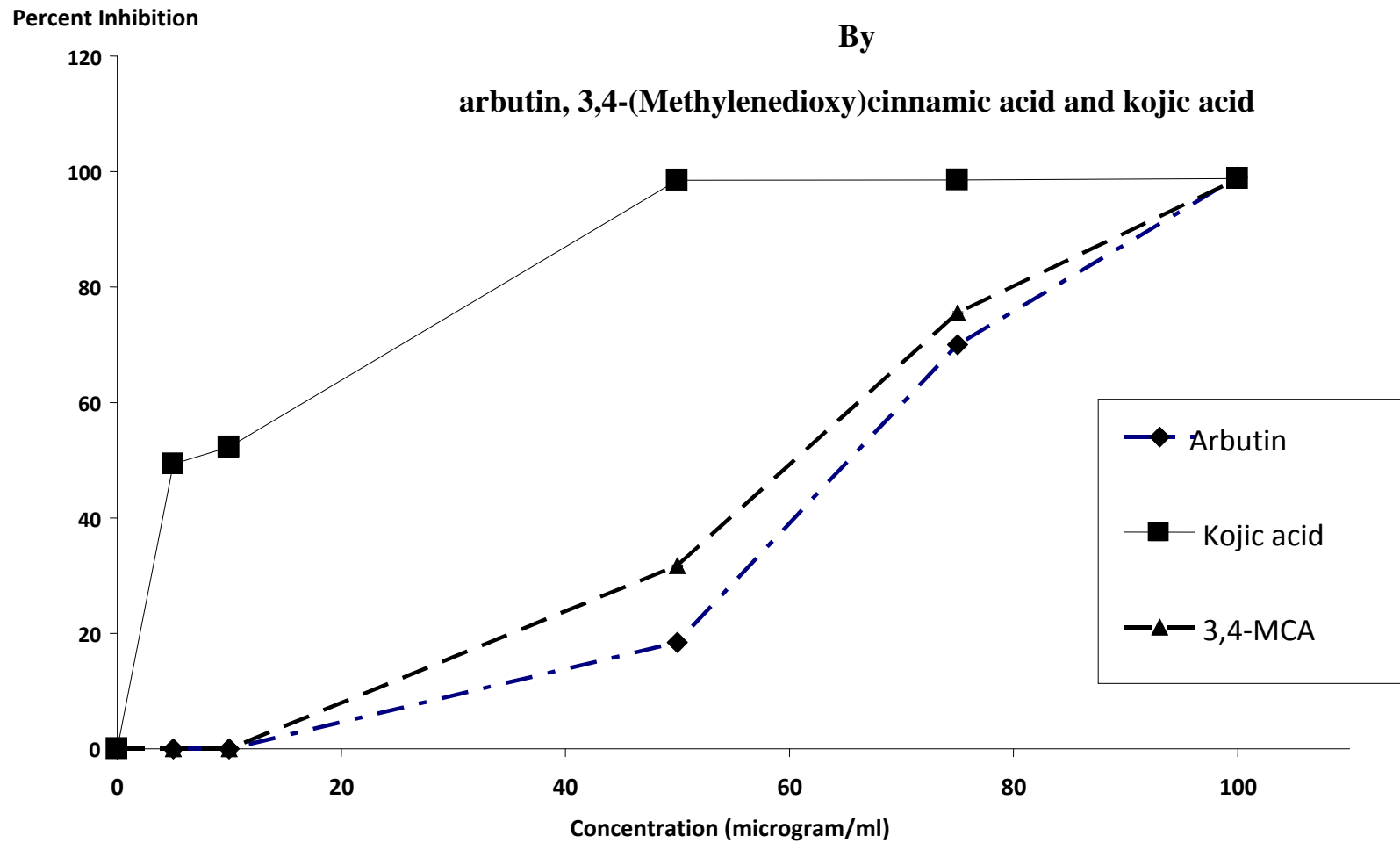
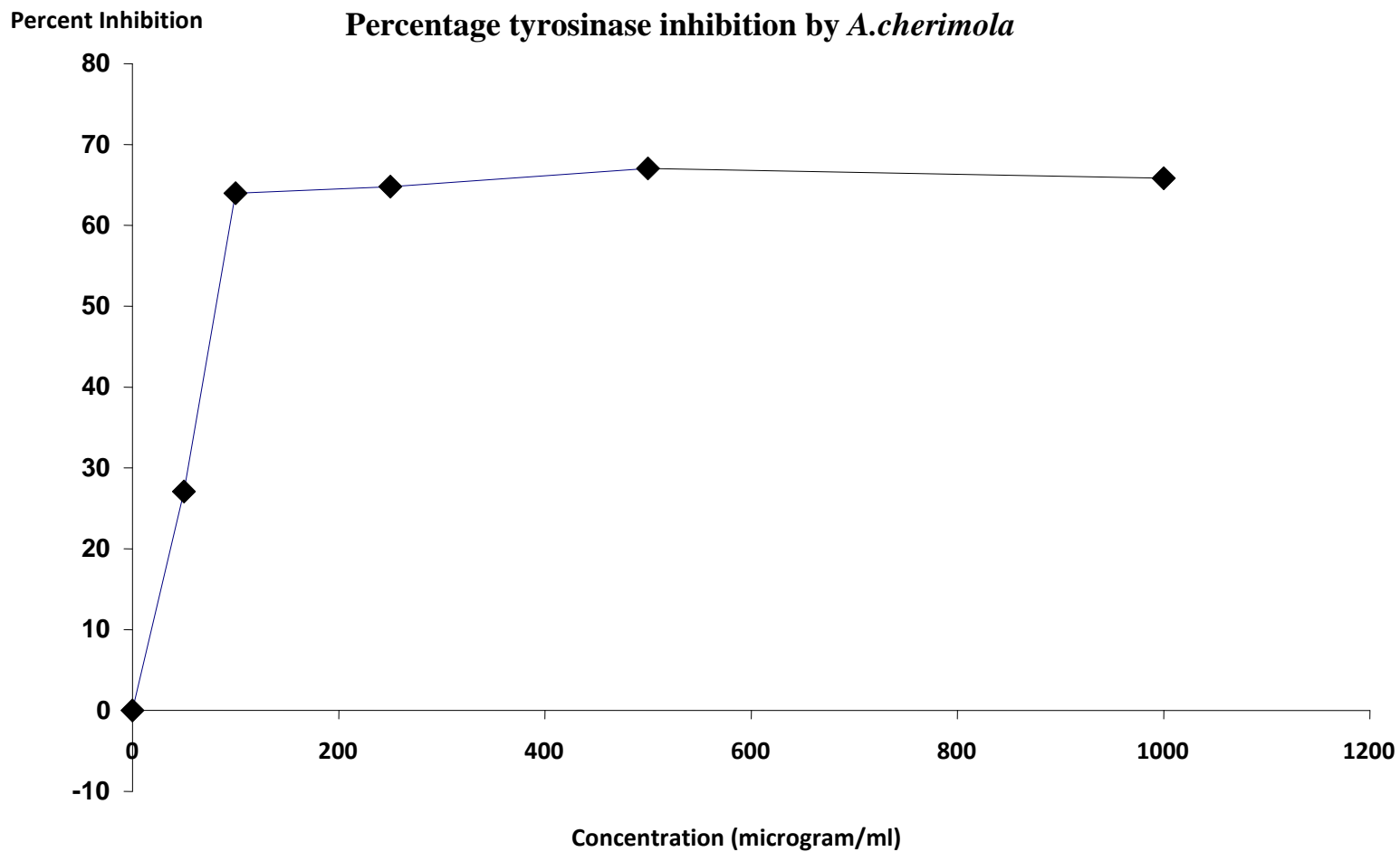


Figure 15



6. References

Ahmad V U, Ullah F, Hussain J, Farooq U, Zubair M, Khan M, Hassan M, and Choudhary MI.(2004). Tyrosinase inhibitors from *Rhododendron collettianum* and their structure-activity relationship (SAR) studies. **Chemical & Pharmaceutical Bulletin**; 52: 1458–1461.

Alijanianzadeh M, Saboury A, Mansuri-torshizi H, Haghbeen K, Moosavi-movahedi A (2007). The inhibitory effect of some new synthesized xanthates on mushroom tyrosinase activities. **Journal of Enzyme Inhibition and Medicinal Chemistry**, 22(2): 239–246.

Ariens, A. (1966). A Basis for Drug Design. Progress Drug Research, **Molecular Pharmacology**, 10: 429.

Arung, Enos Tangke; Kusuma, Irawan Wijaya; Iskandar, Yetti Mulyati; Yasutake, Seiji; Shimizu, Kuniyoshi and Kondo, Ryuichiro (2005). Screening of Indonesian plants for tyrosinase inhibitory activity, **Journal of Wood Science**, 51(5), 520-525.

Battaini, G., Monzani, E., Casella, L., Santagostini, L., Pagliarin, R. (2000). Inhibition of catecholase activity of biomimetic dinuclear copper complexes by kojic acid. **J. Bio. Inorg. Chem.**, 5: 262-268.

Bran, R., and Maibach, H., (1994). Cosmetic dermatology. (1ST ed.), United Kingdom: Martin Dunitz.

Breathnach AC. (1989). Azelaic acid therapy in disorders of pigmentation **Clinics In Dermatology**, 7: 106–119.

Briganti S, Camera E, Picardo M (2003). Chemical and instrumental approaches to treat hyperpigmentation. **Pigment Cell Research**; 16: 101-110.

Casan˜ola-,Martı´n GM, Marrero-Ponce Y, Khan M, Ather A, Sultan S, Torrens F, Rotondoh R. (2007). TOMOCOMD-CARDD descriptors-based virtual screening of tyrosinase inhibitors: Evaluation of different classification model combinations using bond-based linear indices. **Bioorganic & Medicinal Chemistry**; 15: 1483-1503

Catalyst User Guide, (2005) Accelrys Software Inc., San Diego.

Chen, Y., Chavin, W. (1978). In vitro effects of melanocytolytic agents and other compounds upon dominant human melanoma tyrosinase activity. **Experientia**, 34(1), 21-2.

Choi, Yeong; Kim, Sun Gyeom; Park, Gyeong Chan. (2003). Whitening composition containing *rhodiola rosea* extract. Patent written in Korean. Application: KR 2001-46636 20010801.

Clement, O.O & Mehl, A.T. in: Guner F.O. (Ed.), (2000). Pharmacophore perception, development and use in drug design-IUL Biotechnology Series, **International University Line, La Jolla**, California, 71–84.

Cohen, N.C. (1996). Guidebook on Molecular Modeling in Drug Design. Academic Press, UK.

Creager, J.G. (1992). Human anatomy and physiology, (2nd ed.), United State of America: Brown Publisher.

Crippon, G.M. (1977). A novel approach to calculation of conformation, distance Geometry. **J.of Computational Physics**, 24: 96-107.

Curto V& Kwong C. (1999). Inhibitors of mammalian melanocyte tyrosinase: in vitro comparisons of alkyl esters of gentisic acid with other putative inhibitors. **Biochemical Pharmacology**; 57: 663-672.

Curto, E.V., Kwong, C., Hermersdorfer H., Glatt, H., Santis, C., Virador, Hearing, V.J., Dooley, and T.P. (1999). Inhibitors of mammalian melanocyte tyrosinase: in vitro comparisons of alkyl esters of gentisic acid with other putative inhibitors. **Biochem. Pharmacol**, 57: 663-672.

De Caprio, A.P. (1986). The toxicology of hydroquinone-relevance to occupational and environmental exposure. **Crit. Rev. Toxicol.**, 29: 283-330,

Decker H, Schweikardt T, Tuzek F. (2006). The First Crystal Structure of Tyrosinase: All Questions Answered? **Angewandte Chemie International Edition**. 45: 4546 - 4550.

Devkota K P, Khan MT, Ranjit R, Lannang AM, Samreen, Choudhary M I. (2007). Tyrosinase inhibitory and antileishmanial constituents from the rhizomes of Paris polyphylla. **Natural Product Research** 21(4): 321–327.

Dothan, N. F., (1978). Ericacea to Compositae. Flora of Palaestina, (3 ed.), Jerusalem: Israel academy of sciences and humanities.

Fitzpatrick T.B. & Breathnach A.s, (1963). The epidermal melanin unit system, **Dermatol Wochenschr**. 18; 147:481-9.

Friedman MJ. (1996). Food Browning and Its Prevention: An Overview. **Journal of Agricultural and Food Chemistry**; 44:631-653.

Fritsch, P. (1990). **Dermatologie**. 3. Auflage. Springer-Verlag.

Garcia, A., Fulton, J.E. (1996). The combination of glycolic acid and hydroquinone or kojic acid for the treatment of melasma and related conditions. **Dermatol. Surg.**, 22: 443-447.

Green, J., Kahan, S., Savoj, H. Sprague, P. and Teig, S. (1994). Chemical Function Queries for 3D Database search. **J.Chem.Inf.Comput.Sci**, 34:1297-1308.

Griffiths CEM, Finkel LJ, Ditre CM, Hamilton A, Ellis CN, Voorhees JJ. (1993). Topical tretinoin (retinoic acid) improves melasma. A vehicle-controlled, clinical trial. **The British Journal of Dermatology**, 415–421.

Gund, P. (1977). Three Dimensional Pharmacophoric Pattern Searching. In: Progress in Molecular and Subcellular Biology. Hahn, F.E., vol. 5, Springer-Verlag, Berlin.

Gund, P. Wipke W.T, Langridge R, (1974). Computer searching of a molecular structure file for pharmacophoric patterns. In: Proc Intl. Conf on Computers in Chem Res and Educa. Elsevier, Amsterdam.

Hahn (1997).Three-Dimensional Shape-Based Searching of Conformationally Flexible Compounds. **J.Chem.Inf.Comp. Sci**, 37: 80-86.

HipHop User Guide Version 3.1, Catalyst 4.10, Accelrys Inc., San Diego, CA, 2005 (www.accelrys.com/doc/life/catalyst410/help/hipHop/HipHop_23TOC.doc.htm).

Hira, Y., Hatae, S., Inoue, T., Ohyama, Y. (1982). Inhibitory effects of kojic acid on melanin formation. In vitro and in vivo studies in black goldfish. **J. Jap. Cosmetic Sci. Soc.**, 6: 193-194.

Hoi-Seon Lee (2002). Tyrosinase Inhibitors of Pulsatilla cernua Root-Derived Materials. **J. Agric. Food Chem.** 50, 1400-1403.

Hori I, Nihei K and Kubo I (2004). Structural criteria for depigmenting mechanism of arbutin. **Phytother Res**, 18(6):475-9.

In Proceedings of the 9th European CATALYST User Group Meeting, Advanced Seminars in CATALYST Frankfurt, Germany, March (2006), Accelrys Inc., San Diego, CA, 2006.

Iozumi K, Hoganson GE, Pennella R, Everett MA and Fuller BB J (1993). Role of tyrosinase as the determinant of pigmentation in cultured human melanocytes. **Journal of Investigative Dermatology**; 100: 806-811.

Jaenicke, E and Decker, H. (2003). Tyrosinases from crustaceans form hexamers. **Biochem. J.** 371: 515-523.

Jeong-Yeon Lim, Kyoko Ishiguro and Isao Kubo (1999). Tyrosinase Inhibitory p-Coumaric Acid from Ginseng Leaves. **Phytotherapy Research** 13, 371–375.

Jimbow K, Quevedo WC Jr, Fitzpatrick TB, Szabo G (1976). Some aspects of melanin biology: 1950-1975. **J Invest Dermatol.** 67(1):72-89.

Jin-Mi N, Seon-Yeong K, Do-Hyun K, Yoon-Sik L (2007). Kojic Acid–Tripeptide Amide as a New Tyrosinase Inhibitor. **Biopolymers (PeptideScience)** 88(2): 300–307.

Josefa E., Fernando,G., Nuria C. and Maria A. (2002). Subcellular Localization and Isoenzyme Pattern of Peroxidase and Polyphenol Oxidase in Beet Root (Beta vulgaris L.) **J. Agric. Food Chem.** 50, 6123–6129.

Jun N, Hong G and Jun K (2007). Synthesis and evaluation of 20, 40, 60-trihydroxychalcones as a new class of tyrosinase inhibitors. **Bioorganic & Medicinal Chemistry**; 15: 2396–2402.

Kaminski, J.J, Rane, D.F, Snow, M.E, Weber, L., Anderson S.D and Lin S.L, (1997). Identification of novel Farnesyl protein transferase inhibitors using three dimensional database searching methods. **J.Med.Chem**, 40(25): 4103-4112.

Kaufman, J. and Karman, E. (1974). Quantum Chemical and other theoretical techniques for the understanding of the psychoactive action of phenothiazines. In: The phenothiazines and structurally related drugs. Forrest. I.S., C.J, Usden, Raven, New York, USA.

Kamya, Shintaro; Nakagawa, Yoshuki; Sasuga, Keiji. (1994). Skin-lightening cosmetics containing (+)-catechin glycosides and preparations of the glycosides. Patent written in Japanese. Application: JP 92-212126.

Khan MT, Choudhary MI, Khan KM, Rani M, Attaur R. (2005). Structure-activity relationships of tyrosinase inhibitory combinatorial library of 2,5-disubstituted-1,3,4-oxadiazole analogues. **Bioorganic & Medicinal Chemistry** 13: 3385-3395.

Khatib S, Nerya O, Musa R, Shmuel M, Tamir S, Vaya J. (2005). Chalcones as potent tyrosinase inhibitors: the importance of a 2, 4-substituted resorcinol moiety. **Bioorganic & Medicinal Chemistry**, 13(2): 433-441.

Kim D, Jeong Y, Park I, Hahn H, Lee H, Kwon S, Jeong J, Yang S, Sohn U, Park K. (2007). A New 2-Imino-1,3-thiazoline Derivative, KHG22394, Inhibits Melanin Synthesis in Mouse B16 Melanoma Cells. **Biological and Pharmaceutical Bulletin**. 30(1): 180-183

Kim YJ, Uyama H. (2005). Tyrosinase inhibitors from natural and synthetic sources: Structure, inhibition mechanism and perspective for the future. **Cellular and Molecular Life Sciences** 62(15):1707-1723.

Kinbrough-Green CK, Griffiths CEM, Finkel LJ, Hamilton TA, Burengo-Ransby SM, Ellis CN and Voorhees JJ. (1994). Topical retinoic acid (tretinoin) for melasma in black patients. A vehicle-controlled clinical trial. **Archives of Dermatology**, 130, 727–733.

Kobayashi Y, Kayahara H, Tadasa K, Tanaka H. (1996). Synthesis of N-kojic-amino acid and N-kojic-amino acid-kojiolate and their tyrosinase inhibitory activity. **Bioorganic & Medicinal Chemistry Letters**, 6: 1303–1308.

Kubinyi HJ (2002). Chemical similarity and biological activities. **Journal of the Brazilian Chemical Society**; 13: 717–726.

Kubo I, Chen Q, Nihei K. (1999). Molecular design of antibrowning agents: antioxidative tyrosinase inhibitors. **Food Chemistry** 2003; 81: 241- 247.

Kubo I and Kinst-Hori IJ (2000). Flavonols from saffron flower: tyrosinase inhibitory activity and inhibition mechanism. **Journal of Agricultural and Food Chemistry** 47: 4121–4125.

Kurogi, Y. and Güner, O. F. (2001). Pharmacophore modeling and three-dimensional database searching for drug design using catalyst. **Curr. Med. Chem.** 8, 1035-1055.

Kwak, M.Y., Rhee, J.S. (1992). Cultivation characteristics of immobilized *Aspergillus oryzae* for kojic acid production. **Biotechnol. Bioeng.**, 39: 903-906,

Lee, K.T, Kim, B.J & Kim, J.H. (1997). Biological screening of 100 plant extracts for cosmetic use (I): inhibitory activities of tyrosinase and DOPA auto-oxidation. **International Journal of Cosmetic Science** 19, 291–298.

Lee, L.S., Parrish, F.W., Jacks, T.J (1999). Substrate depletion during formation of aflatoxin and kojic acid on corn inoculated with *Aspergillus flavus*. **Mycopathologia**, 93: 105-107.

Lee, O.S., and Kim, E-J. (1995). Skin lightening. **Cosmetics & Toiletries magazine**, 110: 51-56.

Li W & Kubo I. (2004). QSAR and kinetics of the inhibition of benzaldehyde derivatives against *Sarcophaga neobelliaris* phenoloxidase. **Bioorganic & Medicinal Chemistry**, 12: 701-713.

Lim, J.T. (1999). Treatment of melasma using kojic acid in a gel containing hydroquinone and glycolic acid. **Dermatol. Surg.**, 25: 282-284.

Lin Y, Hsu F, Chen C, Chern J, Lee M. (2007). Constituents from the Formosan apple reduce tyrosinase activity in human epidermal melanocytes. **Phytochemistry**, 68: 1189-1199

Lipinski C.A, (2004). Lead- and drug-like compounds: the rule-of-five revolution, **Drug Discov. Today: Technol.** 1, 337–341.

M.A. DePristo, P.I.W. de Bakker, T.L. Blundell (2004). Heterogeneity and inaccuracy in protein structures solved by X-ray crystallography, *Structure* 12 831–838.

Maeda K, Naitou T, Umishio K, Fukuhara T, Motoyama A (2007). A novel melanin inhibitor: hydroperoxy traxastane-type triterpene from flowers of *Arnica montana*. **Biological & Pharmaceutical Bulletin**; 30(5): 873-879.

Maeda, K., Fukuda, M. (1996). Arbutin: mechanism of its depigmenting action in human melanocyte culture. **J. Pharmacol. Exp. Therapeutics.**, 276: 765-769.

Masuda, M.; Tejima, T.; Suzuki, T. and Imokawa, G., (1996). Skin Lighteners. **Cosmetics & Toiletries Magazine**, 111:65-77.

Matoba Y, Kumagi, T. (2006). Crystallographic evidence that the dinuclear copper center of tyrosinase is flexible during catalysis. **J. Biol. Chem.** 281 (13): 8981-8990.

Matsuda, H., Nakamura, S., Shiimoto, H., Tanak, T., and Kubo, M. (1992). Pharmacological studies on leaf of *Arctostaphylos uva-ursi* (L.) Spreng. IV. Effect of 50% methanolic extract from *Arctostaphylos uva-ursi* (L.) Spreng (Bearberry leaf) on melanin synthesis. (in Japanese) **Yakugaku-Zasshi**. 112: 276-282.

Mayer AM (2006). Polyphenol oxidases in plants and fungi: Going places? A review. **Phytochemistry** 67: 2318-2331.

Miyazawa M, Oshima T, Koshio K, Itsuzaki Y and Anzai J. (2003). Tyrosinase inhibitor from black rice bran. **Journal of Agricultural and Food Chemistry** 51: 6953-6956.

Miyazawa M, Tamura N. (2007). Inhibitory Compound of Tyrosinase Activity from the Sprout of *Polygonum hydropiper* L. (Benitade). **Biological and Pharmaceutical Bulletin**; 30(3): 595-597.

Moon, K.Y., Ahn, K.S., Lee, J.S., Kim, Y.S. (2001). Kojic acid, a potential inhibitor of NF-kappa B activation in transfectant human HaCaT and SCC13 cells. **Arch. Pharm. Res**, 24: 307-311.

Mosher, D.B., Fitzpatrick, T.B., and Ortonne, J.P., (1987). Disorders of melanocytes .In: Fitzpatrick, T.B.; Eisen, A.Z., and Wolff K , *Dermatology in general medicine*, (5th ed.), 810-854 , New York: McGraw-Hill.

N.R.A. Beeley, C. Sage (2003). GPCRs: an update on structural approaches to drug discovery, **Targets**, 2: 19–25.

Nakagawa, M., Kawai, K., Kawai, K. (1995). Contact allergy to kojic acid in skin care products, **Contact Dermatitis**, 32: 9-13.

Nakagawa, Akira; Takahashi, Senji, (2004). Melanogenesis inhibitory substances. Patent written in Japanese. Application: WO 2004-JP5642 20040420

Nazzaro-Porro, Marcella; Passi, Siro (1978). Identification of tyrosinase inhibitors in cultures of *Pityrosporum*. **Journal of Investigative Dermatology** 71(3), 205-8.

Neering, H. (1975). Treatment of melasma (chloasma) by local application of a steroid cream. **Dermatologica**, 151, 349–353.

Nicolay, J., F., and Levrat, B., (2003) .A keratinocytes- melanocytes coculture system for the evaluation of active ingredients effects on UV-induced melanogenesis. **International Journal of Cosmetic Science**, 25: 15-19.

Nihei K and Kubo I. (2003). Identification of oxidation product of arbutin in mushroom tyrosinase assay system. **Bioorganic & Medicinal Chemistry Letters** 13: 2409-2412.

Nordlund JJ, Boissy RE, Hearing VJ, King RA, Ortonne JP, (1998). Pigmentary System. In: Physiology and Pathophysiology. Oxford University Press, Oxford.

Nose, Taisuke; Miki, Wataru. (1994). Tyrosinase inhibitors containing phenols. Patent written in Japanese. Application: JP 92-263926 19921001.

Ohyama Y & Mishima Y. (1990). Melanogenesis-inhibitory effect of kojic acid and its action mechanism. **Fragrance Journal**, 6, 53-58.

Ohyama, Y. and Mishima, Y, (1990). Melanogenesis-inhibitory effect of kojic acid and its action mechanism. **Fragrance J**, 18: 53-58,

Okunji C, Komarnytsky S, Fear G, Poulev A, Ribnicky DM, Awachie PI, Ito Y and Raskin I. (2007). Preparative isolation and identification of tyrosinase inhibitors from the seeds of *Garcinia kola* by high-speed counter-current chromatography. **Journal of Chromatography**; 1151: 45–50.

Palumbo, A., D'ischia M, Misuraca G and Porta, G. (1999). Mechanism of inhibition of melanogenesis by hydroquinone. **Biochem. Biophys. Acta**, 23: 85-90.

Curto, E.V., Kwong, C., Hermersdorfer H., Glatt, H., Santis, C., Virador, V., Hearing, V.J. and Dooley, T.P (1999). Inhibitors of mammalian melanocyte tyrosinase: in vitro comparisons of alkyl esters of gentisic acid with other putative inhibitors. **Biochem. Pharmacol**, 57: 663-672.

Palumbo, A., D'ischia, M., Misuraca, G., Prota, G. (1992). Skin depigmentation by hydroquinone: a chemical and biochemical insight. **Pigment Cell Res. Suppl.**, 2: 299-303.

Passi, S. And Nazzaro-Porro, M, (1981). Molecular basis of substrate and inhibitory specificity of tyrosinase: phenolic compounds. **Br. J. Dermatol.**, 104: 659-665.

Pastor M., G. Cruciani and K. Watson, (1997). A strategy for the incorporation of water molecules present in a ligand binding site into a three-dimensional quantitative structure–activity relationship analysis, **J. Med. Chem.** 40: 4089–4102.

Pawelek, J.M. and Chakraborty, A.K, (1998). The Enzymology of Melanogenesis, In: The pigmentary system: physiology and pathophysiology, Nordlund J.J., Boissy R.E., Hearing V.J., King R.A., Ortonne J.P. (Eds.). New York, Oxford university press, 391- 400.

Penney K.B., Smith C.J. and Allen, J.C. (1984). Depigmenting action of hydroquinone depends on disruption of fundamental cell processes. **J. Invest. Dermatol.**, 82: 308-310.

Pérez-Bernal, A., Muñoz- Pérez, M.A. and Camacho, F. (2000). Management of facial hyperpigmentation. **Am. J. Clin. Dermatol.**, 1(5): 261-268.

Petroni, P.C, (1986). Alternative medicine. **Practitioner**; 230:1053-1054.

Poncea YM, Khan M, Martina G, Atherf A, Sultankhodzhaevg MN, Torrens F, Rotondoh R and Alvaradoi YJ(2007). Atom-Based 2D Quadratic Indices in Drug Discovery of Novel Tyrosinase Inhibitors: Results of In Silico Studies Supported by Experimental Results. **QSAR & Combinatorial Science**; 26(4): 469 – 487.

Prezioso JA, Epperly MW, Wang N and Bloomer WD (1992). Effects of tyrosinase activity on the cytotoxicity of 4-S-cysteaminyphenol and N-acetyl-4-S-cysteaminyphenol in melanoma cells. **Cancer Letters** 63:73 - 79.

Pruidze, G. N.; Grigorashvili, G. Z. (1975). Properties of the o-diphenol oxidase of table beet roots, Publisher: "Metsniereba", Tiflis, USSR, 44-52.

Prota, G., (1996). Melanins and melanogenesis. **Cosmetics & Toiletries Magazine**. 111: 43-51.

Prota, G., D'ischia, M. and Napolitano, A. (1998). The chemistry of melanins and related metabolites. In: The pigmentary system: physiology and pathophysiology, Nordlund J.J., Boissy R.E., Hearing V.J., King R.A., Ortonne J.P. (Eds.). New York, Oxford University Press, 307-332.

Quevedo, W.G.; Fitzpatrick, T.B.; and Szabo, G., (1987). Biology of the melanin system. In: Fitzpatrick, T.B; Eisen, A.Z, and Wolff K. Dermatology in general medicine. (3rd ed.), 227-258, New York: McGraw-Hill.

Ray K, Chaki M and Sengupta M. (2007). Tyrosinase and ocular diseases: Some novel thoughts on the molecular basis of oculocutaneous albinism type 1. **Progress in Retinal and Eye Research**; 26: 323–358.

Robb D, (1984).Tyrosinase. In: R. Lontie, Editor, Copper proteins and copper enzymes.vol. 2. CRC Press. Boca Raton. FL; 207–241.

Seiberg, M. (2001). Keratinocyte–Melanocyte interactions during melanosome transfer. *Pigment Cell Research* 14: 4 236-242.

Seifert H, Wolf K and Vitt D (2003). Virtual high-throughput in silico screening. **Drug Discovery Today: Biosilico**; 1: 143-149.

Serra-Baldrich, E., Tribó, M.J. and Camarasa, J.G, (1998). Allergic contact dermatitis from kojic acid. **Contact Dermatitis**, 39: 86

Sheridan R.P and Kearsley S.K, (2002). Why do we need so many chemical similarity search methods? **Drug Discov. Today** 7: 903–911.

Shimizu K, Kondo R and Sakai K (2000). Inhibition of tyrosinase by flavonoids, stilbenes, and related 4-substituted resorcinols. Structure-activity investigations. **Planta Medica**; 66: 11–15.

Shin NH, Ryu SY, Choi EJ, Kang SH, Chang IM, Min KR and Kim Y. (1998). Oxyresveratrol as the potent inhibitor on dopa oxidase activity of mushroom tyrosinase. **Biochemical and biophysical research communications**, 243: 801-803.

Singh J, Chuaqui C.E., P.A. Boriack-Sjodin, W.-C. Lee, T. Pontz, M.J. Corbley, H.-K. Cheung, R.M. Arduini, J.N. Mead, M.N. Newman, J.L. Papadatos, S. Bowes, S. Josiah and L.E. Ling (2003). Successful shape-based virtual screening: the discovery of a potent inhibitor of the type I TGF β receptor kinase (TbRI), **Bioorg. Med. Chem. Lett.** 13: 4355–4359.

Smellie A, Kahn S.D. and Teig S.L. (1995). Analysis of conformational coverage. Part 1. Validation and estimation of coverage, **J. Chem. Inf. Comput. Sci.** 35: 285–294.

Smellie A., S. Teig, P. and Towbin, P. (1995). Promoting conformational variation, **J. Comp. Chem.** 16:171–187.

Smellie, A.; Teig, S. Towbin, P. (1995). Promoting conformational variation, **Journal of Computational Chemistry** 16: 171-187.

Song S, Lee H, Jin Y, Ha Y, Bae S, Chungb H, Suha H (2007). Syntheses of hydroxy substituted 2-phenyl-naphthalenes as inhibitors of tyrosinase. **Bioorganic & Medicinal Chemistry Letters**; 17: 461–464.

Sprague P.W., Hoffmann R., in: Waterbeemd H. Van de, Testa B. and Folkers G (1997). (Eds.), *Computer Assisted Lead Finding and Optimization—Current Tools for Medicinal Chemistry*, VHCA, Basel, 230–240.

Spritz RA. And HearingVJ, (1994).Genetic Disorders of Pigmentation. In: *Advances in Human Genetics*. New York, Plenum Press.

Sugumaran M. (1991). Molecular mechanisms for mammalian melanogenesis. Comparison with insect cuticular sclerotization. **FEBS Letters**; 293: 4–10.

Sutter J, Güner O, Hoffmann R, Li H, Waldman M. in: Güner O. F. (2000). Pharmacophore perception, development, and use in drug design, **International University Line**, California, 501-511.

Taha M, Al-Bakri, Amal G.; Zalloum, Waleed A, (2006). Discovery of potent inhibitors of Pseudomonas quorum sensing via pharmacophore modeling and in silico screening. **Bioorganic & Medicinal Chemistry Letters** (22): 5902-5906.

Taha M, Bustanji Y, Al-Bakri A, Yousef A, Zalloum W, Al-Masri I, Atallah N (2007). Discovery of new potent human protein tyrosine phosphatase inhibitors via pharmacophore and QSAR analysis followed by in silico screening. **Journal of Molecular Graphics & Modelling** 25(6): 870-884.

Tazawa, Shigemi; Warashina, Tsutomu; Noro, Tadataka, (2001). Tyrosinase inhibitors of Brazilian propolis. **Natural Medicines**, Journal written in Japanese, 55(3), 111-118.

Theos A.C, Danièle Tenza, José A. Martina, Ilse Hurbain, Andrew A. Peden, Elena V. Sviderskaya, Abigail Stewart, Margaret S. Robinson, Dorothy C. Bennett, Daniel F. Cutler, Juan S. Bonifacino, Michael S. Marks and Graça Raposo, (2005). Functions of Adaptor Protein (AP)-3 and AP-1 in Tyrosinase Sorting from Endosomes to Melanosomes by in Molecular Biology of the Cell, Volume 16, 5356–5372.

Tokiwa, Yutaka; Raku, Takao (2006). Radical scavengers, tyrosinase inhibitors, and cosmetics containing them. Patent written in Japanese. Application: JP 2004-196348 20040702.

Um SJ, Park MS, Park SH, Han HS, Kwon YJ and Sin HS (2003). Synthesis of new glycyrrhetic acid (GA) derivatives and their effects on tyrosinase activity, **Bioorganic & Medicinal Chemistry**; 11: 5345-5352.

Vanni, A., Gastaldi, D. and Giunata, G. (1990). Kinetic investigations on the double enzymatic activity of the tyrosinase mushroom. **Annali di Chimica**. 80, 35–60.

Verallo-Rowell, V. M. (1989). Double-blind comparison of azelaic acid and hydroquinone in the treatment of melasma. **Acta dermato-venereologica** 143, 58–61.

Waszkowycz B., in: A.L. Harvey (Ed.), *Advances in Drug Discovery Techniques*, John Wiley & Sons, Chichester, (1998). pp. 150–153. K.F. Koehler, S.N. Rao, J.P. Snyder, in: N.C. Cohen (Ed.), *Guidebook on Molecular Modeling in Drug Design*, Academic Press, San Diego, CA, 1996, 253–255.

Weidenhagen, R.; Heinrich, F. (2006). Tyrosinase of *Beta vulgaris*. **Zeitschrift des Vereines der Deutschen Zucker-Industrie**. 499-538. ISSN: 0373-0212.

Xu J, Hagler A. (2002). Chemoinformatics and drug discovery. **Molecules**; 7: 566–600.

Xu Y, Storkes AH, Freeman WM, Kumer SC, Vogt BA and Vrana KE, (1997). Tyrosinase mRNA is expressed in human substantia nigra. **Molecular Brain Research** 45:159 – 162.

Yasunobu KT, Gordon M, (1959). Mode of action of tyrosinase in: *Pigment Cell Biology*. New York: Academic Press; 583-608.

Zhang C, Lu Y, Tao L, Tao X, Su X, Wei D (2007). Tyrosinase inhibitory effects and inhibition mechanisms of nobiletin and hesperidin from citrus peel crude extracts. **Journal of Enzyme Inhibition and Medicinal Chemistry** 22(1): 83–90.

Zuidhoff, H.W., and Rijsbergen, J. Mvan, (2001). Whitening efficacy of frequently used whitening ingredients. **Allureds Cosmetics& Tiletries Magazine**, 16 (1): 53-59.

Appendix I

Concentration-dependent inhibition of tyrosinase.

1. Kojic acid

Concentration (μ g/ml)	0	5	10	50	75	100
Inhibition%(Trial 1)	0	49.13	52.75	98.33	98.36	98.53
Inhibition%(Trial 2)	0	49.9	51.68	98.45	98.49	99.04
Inhibition%(Trial 3)	0	48.97	52.43	98.74	98.74	98.85
AV	0	49.33	52.29	98.51	98.53	98.81
SD	0	0.41	0.45	0.17	0.16	0.21

2. Arbutin

Concentration (μ g/ml)	0	5	10	50	75	100
Inhibition%(Trial 1)	0	0.01	0.02	18.32	70.32	99.04
Inhibition%(Trial 2)	0	0.02	0.01	18.44	70.6	98.9
Inhibition%(Trial 3)	0	0.01	0.03	18.53	69.05	99.13
AV	0	0.013	0.02	18.43	69.99	99.02
SD	0	0.005	0.01	0.11	0.83	0.12

3,4-(Methylenedioxy) cinnamic acid

Concentration (μ g/ml)	0	5	10	50	75	100
Inhibition%(Trial 1)	0	0	0	31.32	75.32	98.74
Inhibition%(Trial 2)	0	0	0	32.32	75.7	98.9
Inhibition%(Trial 3)	0	0	0	31.53	75.55	98.46
AV	0	0	0	31.72	75.52	98.7
SD	0	0	0	0.43	0.16	0.18

4. A. Cherimola

Concentration (μ g/ml)	0	50	100	250	500	1000
Inhibition%(Trial 1)	0	27.1	63.86	64.98	66.89	65.69
Inhibition%(Trial 2)	0	26.9	63.76	64.91	67.21	65.88
Inhibition%(Trial 3)	0	27.3	64.33	64.43	67.08	65.98
AV	0	27.1	63.98	64.77	67.06	65.85
SD	0	0.2	0.3	0.23	0.16	0.15

تصميم أنموذج دوائي محوسب لأنزيم التايروسينيز المتعلق بتلون الجلد البشري و استعمال
الأنموذج للتفتيش الإلكتروني عن مثبطات جديدة لأنزيم.

إعداد

رشدي (محمد علي) أبو حمدة

المشرف

الدكتور معتصم طه

المشرف المشارك

الدكتور سجي حامد

ملخص

أنزيم التايروسينيز مهم جداً في تصنيع صبغة الميلانين في الجلد. ولمثبطات أنزيم
التايروسينيز أهمية في المجالات الطبية والتجميلية في علاج العديد من حالات زيادة التلون
في الجلد والتي لها آثار نفسية مثل فقدان الثقة بالنفس.

على الرغم من وجود عدد كبير من مثبطات التايروسينيز إلا أن هذه المثبطات يشوبها عدد
من العيوب كأن تكون ضعيفة التأثير ، أو تكون عالية السمية ، أو تكون قاصرة عن الوصول
إلى مكان التأثير. ومع عدم العثور على أي نموذج دوائي محوسب لأنزيم التايروسينيز في
أي من المراجع فإن هذا البحث بدوره يهدف إلى بناء أنموذج دوائي محوسب عالي الجودة
لأنزيم التايروسينيز، ومن ثم عمل تفتيش إلكتروني عن مثبطات لهذا الأنزيم للحصول على
صفات محسنة مثل التأثير العالي ، والسمية قليلة ، والقدرة العالية على الاختراق.

لقد تم التأكد من صحة هذا الأنموذج مخبرياً عن طريق دراسة المثبطات التي تتبأ بها هذا
الأنموذج ، حيث تم التأكد من قدرة 3,4-(Methylenedioxy) cinnamic acid ومستخلص نبات
الأونونا كيرمولا على تثبيط أنزيم التايروسينيز حيث بينت هذه النتائج أن هذه المثبطات التي
تم التنبؤ بها تثبط الأنزيم بطريقة مشابهة لمادة الأربوتين التي تعتبر بدورها مثبطاً معروفاً
لأنزيم التايروسينيز.

ان هذه النتائج تدعم دور هذا الأنموذج للتعرف إلى مثبطات جديدة لأنزيم التايروسينيز.